

To the Graduate Council:

I am submitting herewith a thesis written by Jeffrey Neal Krumm entitled "Calculated Combustion: An Investigation of Electronic Equipment Tenability in Data Center Fires". I have examined the final electronic copy of this thesis for form and content and recommend that it be accepted in partial fulfillment of the requirements for the degree of Master of Science, with a major in Electrical Engineering.

Dr. Gregory Peterson

Major Professor

We have read this thesis
and recommend its acceptance:

Dr. David Ilove

Dr. A.J. Baker

Accepted for the Council:

Anne Mayhew

Vice Chancellor and Dean of Graduate Studies

(Original signatures are on file with official student records.)

Calculated Combustion: An Investigation of Electronic Equipment Tenability in Data Center Fires

**A Thesis
Presented for the
Master of Science
Degree**

The University of Tennessee, Knoxville

**Jeffrey Neal Krumm
August 2004**

DEDICATION

This thesis is dedicated to my family and friends. Thank you for always being there.

ACKNOWLEDGEMENTS

Through the support of several individuals and the culmination of numerous events, this thesis is made manifest. Primarily, I would like to thank my wife, Emily, for her love, encouragement, and steadfast devotion. This would have been an intolerable undertaking without her. I would also like to thank Dr. Peterson, Dr. Ilove, and Dr. Baker for agreeing to serve as my committee and for providing guidance and insight in the completion of this thesis.

ABSTRACT

Fire presents a clear and present danger to computer equipment and generally results in tremendous expense or irreplaceable loss. This study serves as a proof of concept for using computer-based fire modeling to investigate the resilience of typical data center equipment to fire. In this analysis, the National Institute of Standards and Technology's Fire Dynamics Simulator computer-based fire modeling tool is utilized to simulate fire scenarios within a rack-mount-style computer enclosure containing six circuit boards. Outcomes including effects of combustion (heat, mixture fraction, and species generation) and water-based sprinkler suppression are explored. Although the presence of standard water-based sprinkler suppression proves advantageous, it is not consistently effective in terminating this class of combustion. Results indicate that fire's thermal effects constitute the largest impact and ultimately determine component survivability. The use of computer-based simulation proves to be a valuable tool in the ultimate enhancement of electronic equipment tenability.

TABLE OF CONTENTS

Chapter 1: Overview	
1.1: Introduction.....	1
1.2: Historical Context	2
1.3: Scope	7
Chapter 2: Background	
2.1: Computer Fire Hazards	8
2.2: Suppression Systems.....	18
Chapter 3: Software Tools	
3.1: Description and Requirements	31
3.2: Editing	33
3.3: Simulation.....	35
3.4: Computational Software Model	36
Chapter 4: Investigative Approach	
4.1: Overview	43
4.2: Assumptions.....	43
4.3: Experimental Model.....	44
4.4: Parameters.....	45
Chapter 5: Results	
5.1: Overview	50
5.2: Thermal Effects	50
5.3: Mixture Fraction.....	65

5.4: Species.....	65
Chapter 6: Conclusions and Future Work	
6.1: Recommendations	71
References	73
Appendices	78
Appendix A: Fire Factors Affecting Human Tenability.....	79
Appendix B: Summary of Advantages and Disadvantages of Different Fire Extinguishing Systems	82
Appendix C: Partial Listing of Water Misting Technology Interest.....	84
Appendix D: FDS Variable Descriptions.....	85
Appendix E: FDS Default Parameter File Listing for Central K-11 Sprinkler.....	86
Appendix F: Sample FDS Input File Listings.....	87
Vita	94

LIST OF TABLES

Table 1.2.1. Fire Occurrences: Ignition Source.....	6
Table 1.2.2. Fire Occurrences: Property Damage.....	6
Table 2.1.1. Types of Corrosion.....	11
Table 2.1.2. Corrosive Potential Airborne Concentrations.....	13
Table 2.1.3. Effects of Contamination.....	15
Table 2.1.4. Thermal Damage Thresholds.....	17
Table 2.2.1. Wet and Dry Pipe Sprinkler Systems.....	20
Table 2.2.2. Halon Properties.....	24
Table 2.2.3. Human Safety Advantages and Concerns of Water Mist.....	30
Table 4.4.1. Set of Experimental Fire Simulations.....	48

LIST OF FIGURES

Figure 2.2.1. Periodic Table: Halogens	23
Figure 3.2.1. FDS Naming Conventions	34
Figure 4.4.1. Compartment Design	46
Figure 5.2.1. Isosurface Example	51
Figure 5.2.2. Slice File Examples (Normal and Vector)	53
Figure 5.2.3. Boundary File Examples (Temperature, Radiative Flux, and Convective Flux)	54
Figure 5.2.4. Boundary Temperature Measurements (Small HRR)	55
Figure 5.2.5. Boundary Temperature Measurements (Large HRR)	57
Figure 5.2.6. Thermocouple Plot	58
Figure 5.2.7. Heat Release Rate Plot	58
Figure 5.2.8. Radiation Loss Plot	59
Figure 5.2.9. Convection Loss Plot	59
Figure 5.2.10. Conduction Loss Plot	60
Figure 5.2.11. Burn Rate Plot	60
Figure 5.2.12. Ceiling Flame Impingement	62
Figure 5.2.13. Sprinkler Activation and Suppression	63
Figure 5.2.14. Suppressed Thermocouple Plot	64
Figure 5.3.1. Isosurface Mixture Fraction	66
Figure 5.3.2. Slice File Mixture Fraction	67
Figure 5.4.1. Species Plot	69

Chapter 1

Overview

1.1 Introduction

As electronic and computer technology continues to advance, its scope and application grows. With this growth comes a torrent of calculation and data that lends itself to other needs such as processing, storage, retrieval, accessibility—the list is endless. Within the context of the corporate world, the magnitude of these needs expands almost exponentially. Thus enters an army of rack-mounted computer and data storage systems aligned in rank and file performing their duties.

Imagine yourself at the technological helm of a large corporation. As manager of information systems, you are ultimately responsible for the storage and safety of hundreds or thousands of employees' files and data sets. For years, it has been business as usual. Then, one day, someone notices a light on the fire alarm control panel. Before anyone can say a word, the fire alarm claxon sounds and the building is evacuated. Firefighters arrive on the scene and race into the entrances. The atmosphere is charged with conversation and conjecture. You wait for what seems an eternity when, suddenly, the “all clear” signal is sounded and you are permitted to re-enter the building. You immediately head for the data center. Upon entry, to your horror, you stare into the charred and sooty

remains of a once pristine computer room. Two words echo hollowly in your head, “What happened?” Sadly, without appropriate fire suppression and preventative measures, this scenario is an all-too-likely reality. Whether initiated via human interaction, mechanical failure, electrical malfunction, or any of a myriad of possible sources, fire embodies just one of a computer data center’s most devastating foes. Ironically, through mathematical and physical fire modeling, computers are now able to fight back. With the aid of computer fire modeling, one can better visualize and understand the threats that fire presents to electronic equipment.

1.2 Historical Context

Although a distinction between corporate and household electrical fire significance can be drawn with respect to scale, in the end, both types result in physical and financial devastation. To assist in bringing this threat into focus, one may turn to recorded fire data. In household situations alone, Britain’s 1999 fire census shows that 10% of all recorded fire occurrences originated with electrical equipment. These fires account for 19% of the United Kingdom’s fire-related injuries and are the most costly, averaging slightly more than \$7,000 per incident [1]. Canada, in 2000, cites over 7,400 electrically-linked blazes totaling 225,068,279 Canadian Dollars (CAD) [2]. Finally, in the United States, household electrical fires accounted for 38,300 fires in 1998. These fires resulted in 284 deaths, 1,184 injuries, and \$668.8 million in property damages

[3]. More recently, in 2000, U.S. public fire services recorded 1,708,000 fires causing approximately \$11 billion in property damages. Building structure fires account for 505,500 of these incidents and 5,800 are designated as office fires leading to an average of nearly \$130 million in property damages. Of these office fires, 37% were electrical in origin [1]. Bearing these statistics in mind, the vulnerability of data centers and seriousness of electrical and electronic fires may be readily seen via a brief inspection of historical case studies.

Scenarios, like the aforementioned, have been documented world-wide for years. One excellent example of this surfaces in Illinois Bell's Hinsdale Central Office fire affecting over 0.5 million customers [4]. Damaging only 60 minicomputers, the fire's effects rippled on for almost 21-23 days and interrupted several hundred Chicago ATMs, a national motel's regional reservation system, and 166 thousand local and long distance telephone circuits [5]. Although the specific cause is still unknown, the battery backup power system was involved and resulted in an estimated 40-60 million dollars in damages in 1988 [6]. A chilling reality, as demonstrated in the Hinsdale office, is that the fire's scale need not be large to cause significant damage or interruption of service. Another, more recent, instance of destruction in a data center is The Treasury's fire. Serving as a leading economic and financial advising group in New Zealand, The Treasury experienced damages in July 1995 as their main computer room's UPS (Uninterruptible Power Supply) ignited [7]. In case after case, computer fire

damage's pervasiveness can be observed. Additional examples include the 1997 U.S. Army Communications and Electronics Command (CECOM) [8], 1969 Zurich-Hottingen telephone exchange [9], and 1988 Los Angeles First Interstate Bank Building [10] fires. Although relatively benign in comparison, CECOM's Research, Development and Engineering Center suffered computer room damages as a workstation erupted into flame [8]. In the Zurich-Hottingen case, extensive destruction resulted as PVC insulated cables burned and corrosive gases penetrated the building's infrastructure including reinforced steel and concrete [9]. Finally, the First Interstate Bank blaze, labeled as "the high-rise fire you can't put out" and requiring the combined efforts of 383 firefighters and paramedics for over 3.5 hours, destroyed five of the building's 62 floors. The fire's origin is believed to be electrical in nature and resided near a number of personal computers [10]. However, computer data center fires are not solely limited to electrical equipment failure.

Human error, vandalism/arson, and terrorist acts comprise additional threats to data centers. Incidents of human error are typically as simple as incorrect cigarette disposal, unintentional fraying of an A/V cart's extension cord, or a spilled beverage. Although accidental, these mistakes have the potential to result in devastating loss. Equally as destructive, albeit malicious in nature, are vandalism/arson and terrorism. These themes introduce the element of criminal intent, but must be considered. The premeditated incident at Penn Mutual Life

Insurance's data processing facility depicts one such occasion. Initial fire-damage estimates totaled \$8 million which included the loss of two IBM 3081 mainframes, eleven DASD strings, and an unspecified quantity of microcomputers and peripherals [11]. Further illustrations include the 1993 terrorist attack on the World Trade Center. In this instance, non-thermal damage from smoke and corrosive fire products was documented throughout Tower One, including floors 16-90, and necessitated equipment restoration and replacement. In 1990, Karydas surveyed, itemized, and categorized a number of large-loss (greater than \$1 million), non-thermal, fire-related property damage occurrences [12]. These instances and their resulting damages, involving electrical equipment (electrical), flammable/combustible materials (incendiary), tobacco smoking (smoking), and various other ignition sources (miscellaneous), are summarized in Tables 1.2.1 and 1.2.2. This information shows that electrical systems account for over a third of the fires cited and an estimated \$48 million in non-thermal damages alone.

An additional point for consideration is that data center fires do not only result in physical loss. Even when data is not lost, an unexpected fire can pit one against insurmountable odds. Frequently, especially when unforgiving schedules are involved, a resultant loss of service may necessitate project outsourcing and can be more difficult to overcome than merely replacing equipment. The National Weather Service's 1999 computer room fire serves as an occasion where a

Table 1.2.1. Fire Occurrences: Ignition Source [12]

Source	Number of Incidents	Percent of Total
Electrical	10.5	35
Incendiary	7.5	24
Smoking	4.5	15
Miscellaneous	4.0	13
Total	30.0	100

Table 1.2.2. Fire Occurrences: Property Damage [12]

Property	Losses (number)	Losses (\$ Millions)	Percent (number)	Percent (\$)
Electrical	10	48	33	41
Textile	5.0	24	17	21
Building/Equipment	8.5	20	28	17
Merchandise	5.0	13	17	11
Foodstuff	1.5	11	5	10
Total	30	116	100	100

viable solution was achieved through an outsourcing arrangement after losing a CRAY C-90 forecasting supercomputer [13]. However, not all situations work out so favorably.

1.3 Scope

This research investigates the realm of electrical and computer equipment fire tenability. It begins with an overview of available information and provides historical context grounding. The text then continues (in Chapter 2) with an explanation of the various types of computer fire hazards and explores current and previous fire suppression methodologies. After reviewing the inherent dangers, Chapter 3, contains an overview of the National Institute of Standards and Technology's (NIST) software-based fire modeling and analysis tools—Fire Dynamics Simulator (FDS) and Smokeview. Chapter 4 outlines the specific investigative approach and model constructed (including observed parameters and assumptions). Experimental data and outcomes are analyzed in Chapter 5. Finally, Chapter 6, culminates with conclusions and recommendations for future work.

Chapter 2

Background

2.1 Computer Fire Hazards

As alluded to previously, computer fire hazards are not merely limited to thermal exposure. Although intense heat produced by combustion obviously poses a massive threat to the electronic hardware and storage media typically contained in a data center, additional dangers do exist. These dangers include immediate and long-term damaging mechanisms alike. The United States Department of Energy (DOE) organizes these hazards into three primary categories—heat, smoke corrosivity, and soot deposition [4].

Several factors play a part in determining a fire's heat release rate. These elements include the fuel's chemical composition, the fuel's orientation, the room's size and shape, and the room's vent arrangement. Objects within the room are viewed from the fire's perspective as additional fuel sources or targets. Thermal damage can be attributed directly to flame impingement, radiative heat flux, and convection. As a fire continues to burn, its plume forms an upper layer of heated gases. The flames, upper gas layer, compartment walls, and heated surfaces are all sources of radiative heat. Additionally, if a target is immersed within the upper gases, convection increases the thermal intensity and subsequent damage. For materials typically contained in a data center, heat

fluxes of less than 10 kW/m² will not incur auto-ignition [4]. However, temperatures of 79.4°C (175°F) are high enough to damage functioning computer equipment [14]. These heat levels are also sufficient to cause plastic elements such as keyboards, PVC conduits, monitors, cable insulations, printers, or tape backup media to melt or deform. As evidenced by the 1988 Harwell tests conducted in the U.K., computer tapes provide a ready fuel source that enables fires of particularly-high ferocity and tenacity to develop [5]. One source states that temperatures of 75°C (165°F) will ruin tapes and disk packs while temperatures of 55°C (133°F) will damage diskette media [15]. The National Fire Protection Association (NFPA) sets the bar even lower, citing destructive temperatures as low as 37.8°C (100°F) for magnetic and flexible media, with possible successful reconditioning up to 48.9°C (120°F), and 65.6°C (150°F) for disc media [14]. Reconditioning efforts typically involve physical media extraction, cleaning, drying, and duplication within a contaminant-free environment. In the event that temperatures exceed the ignition points of flammable materials within the compartment, flashover occurs. In either a direct flame impingement or a flashover scenario, it is unlikely that any electronic or computer equipment will survive. However, flammable materials aren't the only objects capable of sustaining damage. Inflammable objects, such as metallic racks, computer cases, and hard drives, may still experience mechanical stressing and physical deformation. Factory Mutual's established thermal

thresholds conclude that significant thermal damage may result at temperatures of 175°F (79°C) and malfunction at 140°F (60°C) [16].

One of the less immediate sources of damage is that of corrosion. Operating on the molecular level, the corrosive effects of a fire are more difficult to assess and may not be immediately evaluated. Table 2.1.1 provides a listing of the various types, descriptions, common locations, and causes of corrosion commonly involved. With the introduction of integrated circuits (ICs), the component scale is drastically reduced. As computer technology continues to evolve, circuits and their interconnects are becoming smaller and more compact. Therefore, as these minimizing efforts continue, even a small amount of corrosion can affect a large number of circuit bridges, solder joints, IC packages, and even the circuit board itself. From an engineering perspective, these corrosive effects result in compromises in circuit integrity leading to metal loss, reduced conductivity, current leaks, short circuits, and system failure. However, to an end user, these same effects manifest themselves in the form of component discoloration, “glitchy” operation, data corruption or loss, frustration, and ultimately, repair costs. Given the combustible materials commonly present in computer and electronic equipment (e.g. wiring insulation, PVC, polymethylmethacrylate (PMMA), and various plastics), the generation of a number of corrosive agents is possible. Even small quantities of burning PVC may produce environments capable of damaging electronic equipment [17]. Typical toxic pyrolysis agents

Table 2.1.1. Types of Corrosion [18-22]

Type	Description	Location	Cause
Pitting	Localized surface corrosion in form of divots	Scattered across surface	Uneven distribution of corrosive agent on surface
Crevice	Similar to pitting, corrosive agent pools within junction	Metal and non-metal junction	Aggregated concentration of corrosive agent within small area
Uniform	Equally-distributed surface corrosion	Entire surface	Even distribution of corrosive agent on surface
Two-Metal	In corrosive agent, more corrosion-resistant metal corrodes slower and less resistant faster than if separate	Two dissimilar metal junction	Electron flow is enhanced at junction
Stress	Material under tensile stress subjected to corrosive agent	Stress Imperfections across surface	Stress-induced cracking, tensile stress, larger surface area

include hydrochloric acid (HCl), hydrofluoric acid (HF), hydrobromic acid (HBr), nitric acid (HNO₃), sulfuric acid (H₂SO₄), carboic acid/phenol (C₆H₅OH), and acetic acid (CH₃COOH) [4]. Table 2.1.2 lists some typical acid-forming gases and their corrosive potential airborne concentrations.

Perhaps, the most common corrosive agent found in fires of this nature is HCl. In reality, gas concentrations have been shown to be lower than theoretical yields [23, 24]. In the case of HCl, for example, concentrations do not typically exceed 200-300 ppm. Clean equipment chloride contaminant concentrations are anticipated to be at or less than 10 µg/in² and are typically 30-60 µg/in² after 20 years [4]. These typical levels, however, are further refined depending on organizational use. For example, equipment is classified as “clean” with a chloride level of 14-17 µg/in² for the military; less than 14 µg/in² for IBM; and less than 20 µg/in² for Honeywell. In spite of this variation, it is commonly accepted that chloride contamination levels of 30-50 µg/in² dictate consideration for reclamation [4]. Chloride contamination reconditioning falls into levels: less than 200 µg/in², 200-600 µg/in², and greater than 600 µg/in² where less than 30 µg/in² is considered a typical background concentration [25]. Categorical transitions represent drastic increases in expense and difficulty. Similarly, acceptable sulfate contamination levels have been established at less than 65 µg/in² [4]. However, even trace amounts of corrosive agents may yield troublesome, if not

Table 2.1.2. Corrosive Potential Airborne Concentrations [26]

Gas	Acid (name)	Acid (formula)	Concentration (ppm)
HCl	Hydrochloric	HCl	100
HF	Hydrofluoric	HF	100
NO ₂	Nitrous	HNO ₂	100
NO ₂	Nitric	HNO ₃	100
SO ₂	Sulfuric	H ₂ SO ₄	1,000
CH ₂ COOH	Acetic	CH ₃ COOH	1,000

disastrous, results over time. Table 2.1.3 summarizes general contaminant levels, typical environmental conditions, and expected effects.

Although corrosive gas production is directly related to the type and quantity of fuel source involved, studies have shown that increased heat and even fire retardant additives may actually enhance a fire's corrosive effects [27].

Ultimately, four factors shape the toxins' resultant yields. These elements are: up to 25% of the ions are trapped in charred portions of the target; 25% or more of the ions condense near the fire; soot affects ion release and absorption; and finally, the gases tend to decay in the atmosphere [4]. Lastly, a compartment's humidity serves as a source of enhancement for the corrosive effectiveness of harmful gases. Excessive humidity levels will result in higher corrosive potential. Acting alone, humidity levels of 85% or more will damage magnetic media [15]. However, minimal humidity levels encourage static electricity—a potentially more deadly foe where electronics are concerned. Therefore, electronic salvage processes typically establish guidelines for environments with relative humidity levels of 30% [28].

A third, and final, fire hazard class is soot deposition. Defined as “particulate materials composed of ... carbon, resins, tar, and unburnt fuel,” soot production is a direct function of the fuel source, burning environment, and duration of burn [4]. Soot can be viewed as the airborne “filth” of a fire resulting in discoloration,

Table 2.1.3. Effects of Contamination [4]

Contamination Level		Ambient Conditions/Typical Environment	Effects	
$\mu\text{g}/\text{cm}^2$	$\mu\text{g}/\text{in}^2$		Metal Surfaces	Electronics
Above 77	Above 500	Very reactive; Humidity >50%; Hot plastics fire; Seawater spray	Flash rust; Etched surfaces	Heavy corrosion; Catastrophic failures
Above 30	Above 200	Reactive; Humidity >60%; Medium to heavy smoke	Light rust; Long term	Active corrosion; Short term
Above 16	Above 100	Factory environment; Humidity 30-90% - uncontrolled	Marginal effects; Long term	Moderate corrosion; Long term
Above 8	Above 50	Controlled environment; Humidity 45-55%; Temp 65-75°F	None	Slight surface corrosion; Long term
Above 3	Above 20	Military standard High reliability	None	None

mechanical damage, and electrical shorting of equipment. Its production may be approximated via a ratio of masses of smoke versus fuel. Typical yields range from 0.05 to 0.15 kg per kg of fuel [4]. Due to the incomplete combustion coexistent with low-temperature fires, higher amounts of soot would be expected in fires possessing a lower heat flux than that of more blistering conflagrations. This particulate matter typically affects exposed, mechanical elements such as cooling fans; floppy, magnetic tape, and optical drives; switching relays; analog meters; and peripherals. It can also alter the effectiveness of thermal dissipaters (heat sinks) and constitute a potential fire risk. Measured via Total Petroleum Content (TPC), clean electronic equipment is typically rated at a level of $5 \mu\text{g}/\text{in}^2$ while equipment exceeding values of 50-100 $\mu\text{g}/\text{in}^2$ is cause for concern [29]. As a point of reference, post-fire measurements of soot, chloride, and halogen acid contamination may exceed 5000 $\mu\text{g}/\text{in}^2$ [4].

Based on DOE data, Table 2.1.4 itemizes source, projected temperature range, possible heat flux, and anticipated level of damage for the three primary fire-related hazards. Individually, any of the three fire-related hazards (heat, corrosion, or soot deposition) possesses the potential to dispatch disaster to electronic equipment. Working in concert, as is common in a fire scenario, these three elements most certainly thrive in ruin.

Table 2.1.4. Thermal Damage Thresholds [4]

Source	Temperature (°C)	Heat Flux (kW/m ²)	Damage
Direct Flame Impingement	330-1,070	5-175 (possible) 90-100 (typical)	Unsalvageable
Upper gas layer	Room temp. – 1,000 (postflashover)	Variable	Dependent on temp and oxygen concentration (Unsalvageable for postflashover)
Soot/Corrosive Gas	Lower temps. (e.g., 50)	Variable	Failure or Reduced Reliability

While the focus of this research is equipment rather than human tenability, it is not uncommon for personnel to be present when a fire erupts. An employee's or fire fighter's ability to function may play a critical role in a data center's ultimate survival. Therefore, Appendix A contains additional information related to human fire risks.

2.2 Suppression Systems

Now that the most common damaging aspects of a fire have been explored, this section investigates the previous and prospective approaches implemented in dousing a blaze. It is a startling fact that nearly 50% of computer room fires actually begin outside the room itself [30]. It is, therefore, imperative that the entire building in which a data center is housed be protected by a fire extinguishing system. Even so, one might assume that an effective means of extinguishing a fire is all that is required to protect a data center and its equipment. This supposition, however, is incorrect. Suppression is merely the first gambit in a strategic game against time and the forces of nature.

Fire suppression brings with it a myriad of challenges and trade offs. Initial attempts at electronic fire suppression paralleled the development of the bucket brigade by pitting a fire against gallons of its arch foe, water. Elaborate piping systems began to spring up in data centers everywhere transporting gallons of water to the inferno. However, this strategy revealed an immediate opportunity

for process improvement. Unless equipment is specifically intended for wet environments, shorting will occur if it is energized [31]. Therefore, the first step in extinguishing a data center fire is typically to de-energize the electrical equipment. Ultimately, there are two classes of water-based sprinkler systems—wet pipe and dry pipe. A wet pipe system is composed of a grid of fusible-link sprinkler heads connected by iron piping that is filled with water at all times. A dry pipe system boasts the same grid structure, but possesses an additional water release valve that separates it from its water supply. Instead of water, the piping in a dry pipe system is initially filled with compressed gas (typically air or nitrogen) until a fire is detected and the water release valve is opened. Both systems hold advantages and disadvantages. These virtues and shortcomings are cataloged in Table 2.2.1

Although commonplace, both types of sprinkler systems are limited by three factors: relatively slow reaction time, quantity and method of extinguishment, and installation flexibility. Commonly rated at 71.1°C (160°F), sprinkler heads may allow surrounding air temperatures to reach as high as 260°C (500°F) [32]. Secondly, once a sprinkler system is activated, it must be shut down manually. This allows for excessive amounts of (possibly dirty) water to spew onto electronic equipment. Lastly, due to their method of operation, sprinkler systems are typically limited to ceiling-level installation and don't excel in the protection of plenums above the ceiling or below the floor.

Table 2.2.1. Wet and Dry Pipe Sprinkler Systems [32]

Type	Advantage	Disadvantage
Wet Pipe	Fast-acting; More common; Simplicity; Cheaper	“Dirty” water; Temperature sensitivity (freezing); Fast-acting (in accidental-release scenario)
Dry Pipe	Temperature insensitivity; Can construct elaborate “pre-action” systems	Increased expense; Slower-acting

In an effort to improve response time and accuracy of activation, a myriad of sensing and detection schemes are used to augment sprinkler systems.

Although three primary types of detectors exist, heat, fire/smoke (photoelectric and ionization), and air sampling, only two are employed to give a data center its ability to identify fire [32]. Because heat detectors are slower to react, a suppression system relying on them for activation would allow a fire to grow too large. Therefore, fire and air sampling detectors provide the higher level of effectiveness necessitated in an electronic environment. Within the realm of smoke detectors, the photoelectric variety more aptly recognizes thicker, darker smoke. Meanwhile, ionization detectors are responsive to the hot gases of combustion. Hence, both types are frequently used jointly to enhance the chance of fire discovery. Air sampling detectors, although more expensive, offer much higher sensitivity. Sporting a single chemical analysis element, multiple plastic or copper tubes extend to and terminate in areas of concern. Air samples are then pulled into the analyzer for examination. Through cross zoning (multiple types of sensors in one area) or additive (suppression requires multiple sensor activations) arrangements, highly elaborate fire detection systems may be constructed.

Although addressing the issue of response time, the addition of sensors and detectors does nothing to alleviate a sprinkler system's installation limitations. Therefore, gaseous agents with enhanced penetrative abilities enter the scene.

Carbon dioxide (CO₂) seemed an ideal total flooding alternative to water. By removing the oxygen necessary for combustion, carbon dioxide simply smothers a fire. However, at the concentrations required to extinguish a fire, typically 30%-40%, carbon dioxide also smothers humans which require a minimum of 18% oxygen to breathe. As a result, carbon dioxide systems are typically equipped with a 90 second pre-activation alarm. This fact, in concert with 10 minute extinguishing times and icy blast damage, undermined carbon dioxide's usefulness [15]. Therefore, its use has been relegated to localized applications and portable fire extinguishers.

In an effort to find a less toxic, yet electronic-friendly, gaseous total flooding agent, the halogens were enlisted. Occupying group seventeen of the periodic table (Figure 2.2.1), halogens contain seven electrons in their outer shell and form salts [33]. When a select number of the hydrogen atoms found in hydrocarbons are replaced by members of the halogen family, a halogenated hydrocarbon (also known as a halon) is produced [32]. However, as all isotopes of astatine are radioactive, it is not amenable to this application [34]. Possessing suitable properties (Table 2.2.2), the two derivative agents most commonly employed in electronic fire suppression are Halon 1211 (bromochlorodifluoromethane, CF₂ClBr) and Halon 1301 (bromotrifluoromethane, CBrF₃) [35]. Halon 1211 is two times more effective than carbon dioxide as a portable extinguishing agent, as it exits a compressed container in liquid form



Figure 2.2.1. Periodic Table: Halogens [33]

Table 2.2.2. Halon Properties [32]

Type	Boiling Point	Common Properties	Common Use
Halon 1211	25°F	Gas at room temp.; Leave little or no residue; Not electrically conductive	Portable Extinguisher
Halon 1301	-70°F		Total Flooding

and can be directed and streamed onto a fire from a distance of ten feet or more. However, with its lower boiling point and smaller concentrations necessary to extinguish a fire (approximately 5-7%), Halon 1301 serves as a more effective total flooding agent [32]. Unlike carbon dioxide, Halon 1301 does not rely on “flame cooling” or “oxygen exclusion” to extinguish a fire. Instead, it interacts with the transient combustion products chemically to halt flame propagation [36]. Therefore, the maintenance of adequate Halon 1301 fire-stopping concentrations is critical and it is recommended that a room be well sealed. In fact, due to poor sealing and lack of enclosure integrity tests, the NFPA once calculated that over 50% of the halon installations in the United States alone may be ineffective [15]. In an attempt to compensate for possible compartment leakage, halon flooding systems are typically designed to provide 8-10% concentrations to ensure that, after 10-15 minutes, the necessary 5-7% concentration remains [32]. Under proper conditions, Halon 1301 systems are capable of extinguishing a fire in 60 seconds and normal operation may resume after a brief ventilation period of two hours [30]. However, it is a sobering fact that only 1 in 10 halon discharges actually suppresses a fire with minimal damage [5]. Perhaps the most significant benefit of Halon 1301 is its improved treatment of humans. Although it is not side-effect free, at requisite levels, Halon 1301 will not suffocate people like carbon dioxide. However, typical symptoms do include dizziness, cardiovascular problems, or respiratory discomfort that will pass with the introduction of fresh

air [32]. In extreme concentrations, higher than 10%, some individuals may suffer from irregular heartbeats or central nervous system disorders [30].

Although Halon 1301 once appeared to be a panacea for computer-based fire extinguishment, its expense and additional corrosive and atmospheric concerns have turned the tide. Halon fire suppressants, unfortunately, contribute to the production of harmful corrosive gases mentioned earlier. Hydrogen fluoride (HF) and hydrogen bromide (HBr), for example, produce deleterious results when exposed to printed circuit board protective coatings. Furthermore, the types of components attached to circuit boards impact equipment failure rate. In particular, CMOS (complementary metal oxide semiconductor) samples fail more readily than NMOS (negative-channel metal oxide semiconductor) and TTL (transistor transistor logic) circuits [37]. However, it is of interest to note that magnetic tape seems to possess more resilience to halogenated atmospheres. In tests performed by Ansul, DuPont, Cardox, and Fenwal, hydrogen fluoride concentrations of less than 294 ppm and hydrogen bromide levels of less than 39 ppm did not appear to negatively affect recorded magnetic tape [17]. However, halons also act as de-greasers and will, over time, result in data loss by weakening the bond between the tape's Mylar backing and data layer [5]. Another critically important factor is halon's negative environmental impact. Halon, similar to that of chlorinated fluorocarbons (CFCs) used in aerosol propellants, some solvents, and Freon refrigerants, promotes the deterioration of

Earth's ozone layer. In fact, with ozone depletion potentials of 10 for Halon 1301 and 3 for Halon 1211, as compared to 0.5 for common CFCs, halon is actually more aggressive [15]. After recognizing this fact, almost 50 nations (including the United States) established the Montreal Protocol of 1987. It outlines taxation and usage-reduction guidelines on CFCs (including halon) resulting in near total abandonment by 2005 [32]. Shortly after the Montreal Protocol was established, halon consumption dropped substantially. Oddly enough, this decline is primarily attributed to the use of alternate test methods and the reduction of discharge checks during system installation. Appendix B contains an at-a-glance comparative summary of the advantages and disadvantages of water-based and Halon 1301-based extinguishing systems.

Today, various hybridized systems are being employed to ensure computer room protection. Typical combinations include gas-water hybrids where sprinklers are arranged for maximum in-room coverage and gaseous agents (both carbon dioxide and halon) augment system effectiveness within plenum spaces and select areas where damage and exposure risks are low. Another modern fire suppression technique that has been gaining recognition is water misting. With testing in Heritage Buildings, prospective application in telecommunications facilities, and interest from organizations such as the International Maritime Organization (IMO), the Factory Mutual (FM), and a host of others (Appendix C), water mist systems may become the next hope for computer rooms as well.

Operating in a similar fashion to existing water-based sprinkler systems, mist systems produce much smaller water droplets that aggregate to form a dense fog. Water droplet sizes are typically on the order of 300-400 microns, but may be smaller than 10-30 microns [38]. Another factor benefiting electronic equipment, research has shown that a fire's smoke plume is typically more conductive than the suppressing water mist [39]. This reduces the potential of arcing damage before equipment is de-energized. Although somewhat arbitrarily defined, water mist systems may be divided into four categories: high pressure (7,000 kPa/1,000 psi) with extremely fine droplets, intermediate pressure (690 kPa/100 psi) with high flow, low flow (being tested for aircraft use), and pneumatic (gas-assisted atomization) systems [40]. Demonstration testing performed by the U.K., Europe, and the U.S. have shown that water mist nozzles may be effective in suppressing fire outbursts, especially when placed within electronic equipment racks or between open-door cabinet aisle ways [41]. In fact, tests conducted by Kidde-Fenwal, GTE, and FSI Research demonstrated that, under specific conditions, it is possible to extinguish vertical rack printed circuit board fires within one to two seconds using less than one liter (0.26 gallons) of water [39]. However, misting still suffers from two daunting unknowns: the most successful process involved in extinguishing a fire and the most effective manner of ensuring correct droplet size and transport [40]. It is clear that standardization and testing is needed. In fact, the NFPA defers to full-scale testing as the only reliable method of testing to ensure effectiveness [41].

However, water misting is not without weakness. Table 2.2.3 identifies potential human safety advantages and concerns of water mist systems. Although water mist systems may possess great potential, progress has been slow due to wavering commitment and the existence of other suppression systems.

Equipped with an arsenal of destruction including heat, corrosion, and soot, fire can bring about disaster where electronic equipment is concerned. Fire damage may manifest itself immediately, as in cases of direct flame impingement, or over great lengths of time, where corrosion is encountered. Although fire detection and suppression systems provide a method of battling fires once they occur, a preemptive means of modeling possible fire scenarios and predicting hazards is even more desirable. This type of prognostic environment is precisely where computer fire modeling software tools come into play.

Table 2.2.3. Human Safety Advantages and Concerns of Water Mist [40]

Advantages	Disadvantages
<ul style="list-style-type: none"><li data-bbox="334 317 667 344">• Cool gas temperatures<li data-bbox="334 354 760 422">• Remove toxins and soot from smoke-filled environment	<ul style="list-style-type: none"><li data-bbox="922 317 1430 422">• Acidic gases combined with smaller droplets may allow deep respiratory transport<li data-bbox="922 432 1328 459">• Steam-type injuries possible<li data-bbox="922 470 1398 537">• Reduced visibility possible due to gas layer destratification

Chapter 3

Software Tools

3.1 Description and Requirements

Since National Institute of Standards and Technology's (NIST) public release of Fire Dynamics Simulator (FDS) Version 1 in February 2000, the field of computer fire modeling has advanced substantially. This advancement has resulted in the subsequent releases of Version 2 (December 2001) and Version 3.1 (April 15th, 2003) [42, 43]. These versions, as well as pre-release Version 4, may currently be downloaded from NIST's FDS and Smokeview download page (<http://fire.nist.gov/fds/refs/download.htm>). Based on the Fortran and C programming languages, FDS will function on multiple computing platforms. Several pre-compiled versions already exist for Microsoft Windows or UNIX/Linux-based machines. However, NIST also provides the source code for compilation and porting to additional operating systems.

Although the FDS software package exists as a single, installable package, it is in fact, a combination of two extremely powerful programs. The components are individually recognized as FDS and Smokeview. NIST succinctly defines FDS as "a computational fluid dynamics (CFD) model of fire-driven fluid flow" [42].

Simply stated, FDS performs the intense mathematical calculations involved in simulating a fire-based environment. FDS exists as a command-line-driven

program that requires an input file used to describe the fire scenario. This data file includes parameters such as room and target dimensions, materials, reaction type, and calculation parameters. Its companion piece, Smokeview, provides a three dimensional graphical user interface (GUI) typically used to view FDS's simulation output. In recent versions, Smokeview has been enhanced and endowed with the ability to assist in rapid, point-and-click type generation of fire scenes.

The software's minimum computer requirements are stated as a 1 GHz Pentium III (or equivalent) with 512 MB of RAM [42]. Although these requirements are not outlandish by today's standards, they are important. Processor speed and memory are two of the largest bottlenecks in performing FDS fire calculations and are directly tied to simulation completion time. It may be obvious that a faster processor results in faster calculations. However, inadequate memory sizes will slow even the fastest CPU. As additional calculations occur, further memory is required. Once the portion of RAM allocated to FDS (directly determined by the total system memory capacity) is filled, the memory contents are temporarily stored on the hard drive. This process is known as "swapping" and is one method of virtually increasing a computer's memory capacity. However, this process bogs a computer by increasing its operational overhead. Larger system memory configurations will reduce instances of data swapping. Two additional computer hardware considerations are hard drive storage and

video card functionality. As stated in the FDS user's manual, depending on complexity, it is not uncommon for a single simulation to require one gigabyte (or more) of storage for output files [42]. A simulation's complexity is affected by a number of factors including: computational grid scale, fire size, reaction, and whether or not supplemental elements such as boundary, slice/vector, particle, isosurface, or PLOT3D files are generated. As is common in the realm of computers, faster machines with larger amounts of memory and storage are better suited for the task at hand.

3.2 Editing

Armed with an understanding of appropriate syntax (detailed in the FDS User's Guide), the process of creating and editing an input file is relatively straightforward. In addition to learning FDS syntax, it is also extremely helpful to know the FDS standard naming conventions, as shown in Figure 3.2.1. Although not a requirement, input files typically end with a ".data" extension and define a fire scenario, as previously mentioned. The FDS database is an additional source file possessing the ".data" extension. Serving as more of an informational repository, the database file is included in the FDS installation and need not be edited. Instead, it includes material and reaction-specific information used in performing the fire simulation. These files are merely text files and may be established and altered in any text editor of choice (Notepad, Wordpad, Microsoft

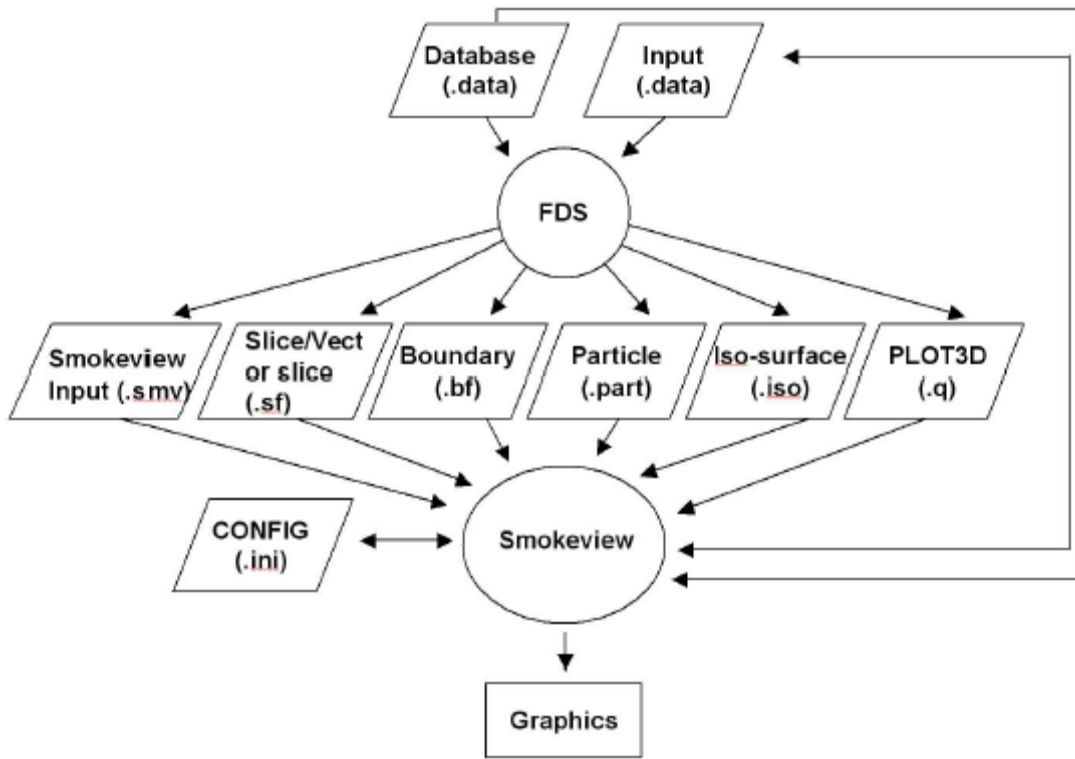


Figure 3.2.1. FDS Naming Conventions [44]

Word, etc.). After the file has been created and the fire scenario has been sufficiently described, simulation may begin.

3.3 Simulation

The act of FDS simulation is also straightforward, assuming a few guidelines are followed. As a command-line tool, FDS begins when instantiated via the `fds3` executable file. However, when called, it does not know the input file name. Therefore, the input data file must be specified when FDS is called. This is accomplished with a command-line operator and looks like *fds3 < inputfile.data*. The less than sign is actually a data redirection operator that sends the input data to FDS. While simulating, FDS generates output including simulation dimensions, time step, parameter calculation, run time messages, and various other values. By default, this output is directed to the screen where it streams by and scrolls into oblivion. However, the default screen output can be redirected, in a similar fashion to the input data, to an output data file via a greater than symbol. Following convention, the output file typically ends with a “.out” extension. All of these operations, the FDS call, input file redirect, and output file redirect, may be accomplished simultaneously on the same command line. The final resulting statement is *fds3 < inputfile.data > outputfile.out*.

In addition to aforementioned screen output, depending on user specifications, FDS may generate a number of data files as shown in Figure 3.2.1. The

Smokeview input file is always generated and serves as the connecting link between FDS and Smokeview. Once executed, Smokeview is capable of opening files with the “.smv” extension and may be directed to load and display any combination of generated FDS output files associated with a particular simulation. These output files include slice/vector slice, boundary, particle, isosurface, and PLOT3D files. Both types of slice files (slice and vector) are positioned via an X, Y, or Z axis location and record cross-sectional simulation data along their specified planar location. Their primary difference is that vector slice files represent direction of motion using vector-based arrows. Boundary files store surface measurements for the compartment’s walls and its contents. Particle files are used to track particle movement including water vapor and element flow. Isosurfaces typically record a fire’s heat release rate per unit area and its mixture fraction (division of smoke and fire). Lastly, PLOT3D files provide simulation snapshots at predefined intervals. In addition to the documented output files, FDS also generates comma-separated-value files denoted by a “.csv” extension. Similar to the scenario input data file, the comma-separated-value files store simulation measurements in plain text format. Therefore, these files may easily be imported into other programs for further analysis.

3.4 Computational Software Model

A detailed analysis of computational fluid dynamic (CFD) theory is beyond the scope of this research. However, this section serves as a cursory introduction to

the fundamentals involved in FDS's computational software model. Further detail and thorough analysis may be found in the FDS Technical Reference Guide [45].

Historically, initial attempts at fire simulation revolved around zone-based fire models. In these representations, a combustion environment is divided into two homogenous levels, a heated upper layer and a cool lower layer, and calculations are performed independently in each layer via algebraic or differential equations. Further information may be found as Quintiere chronicles the zone model's progress through 1983 [46]. Although zone models enjoy widespread implementation, they are limited in that they don't allow for "detailed spatial distributions of physical properties" and can not be systematically improved [42].

The next evolution in computational fire modeling involves the first CFD field models. These models are almost entirely based on work performed by Patankar and Spalding [47]. Specifically, the techniques involved rely on the $k-\epsilon$ turbulence model where k is the turbulent kinetic energy (TKE) and ϵ is the TKE dissipation rate. This model is most commonly cited in Patankar and Spalding's SIMPLE and SIMPLER methods which implement Poisson equations for pressure correction [48].

A more refined version of the field models, the Large Eddy Simulation (LES) CFD model forms the underpinnings of FDS simulation. This methodology finds its grounding in the fundamental Navier-Stokes equations. Explicitly, a simplified version of the Navier-Stokes equations developed by Rehm and Baum, referred to as the “low Mach number” combustion equations, is exploited to reduce computation times. This simplification is realized by filtering out large acoustic variations in temperature and density and results in an elliptic quality that is more characteristic of low-speed convective processes [45].

Established by the user in a scenario’s input data file, FDS divides the fire compartment into smaller, more manageable regions. These regions, or grid cells, determine the resolution of a fire scenario. FDS calculations occur inside each cell of the scenario’s computational grid, are assumed to be uniform within a particular cell, and vary only with time [45]. Beginning with the conservative equations of mass, species, momentum, and energy, NIST uses an approximation of the ideal gas law to relate thermodynamic values. This approximation is referred to as an equation of state and divides overall pressure into three components, background, hydrostatic, and flow-induced perturbation. However, it is noted that the latter two components are relatively small and the background pressure typically dominates. It should be recognized that the energy conservation equation is not directly solved. Instead, its terms give rise to

the divergence constraint equation. Therefore, the resulting simulation equations are:

Conservation of Mass

$$\frac{\partial \rho}{\partial t} + \mathbf{u} \cdot \nabla \rho = \rho \nabla \cdot \mathbf{u}$$

Conservation of Species

$$\frac{\partial \rho Y_i}{\partial t} + \mathbf{u} \cdot \nabla \rho Y_i = -\rho Y_i \nabla \cdot \mathbf{u} + \nabla \cdot \rho D \nabla Y_i + \dot{m}_i'''$$

Conservation of Momentum

$$\frac{\partial \mathbf{u}}{\partial t} + \mathbf{u} \times \boldsymbol{\omega} + \nabla H = \frac{1}{\rho} ((\rho - \rho_\infty) \mathbf{g} + \mathbf{f} + \nabla \cdot \boldsymbol{\tau})$$

Divergence Constraint

$$\nabla \cdot \mathbf{u} = \frac{1}{\rho c_p T} \left(\nabla \cdot k \nabla T + \nabla \cdot \sum_i \int c_{p,i} dT \rho D_i \nabla Y_i - \nabla \cdot \mathbf{q}_r + \dot{q}''' \right) + \left(\frac{1}{\rho c_p T} - \frac{1}{p_0} \right) \frac{dp_0}{dt}$$

Equation of State

$$p_0(t) = \rho T \mathcal{R} \sum_i \frac{Y_i}{M_i} = \frac{\rho T \mathcal{R}}{M}$$

and variable descriptions are included in Appendix D [45]. Before continuing, a few mathematical symbols must be discussed. First, the gradient or grad operator (∇) represents a differential operator with the denotation

$$\nabla = \left(\frac{\partial}{\partial x}, \frac{\partial}{\partial y}, \frac{\partial}{\partial z} \right) = \frac{\partial}{\partial x} \mathbf{i} + \frac{\partial}{\partial y} \mathbf{j} + \frac{\partial}{\partial z} \mathbf{k}, \text{ where } \mathbf{i}, \mathbf{j}, \text{ and } \mathbf{k} \text{ are unit vectors along the } x, y, \text{ and } z \text{ axes.}$$

When used with scalar values, the gradient results in the following

vector equivalence $\nabla\rho = \frac{\partial\rho}{\partial x}\mathbf{i} + \frac{\partial\rho}{\partial y}\mathbf{j} + \frac{\partial\rho}{\partial z}\mathbf{k}$. When applied to vectors, the gradient

results in a tensor or vector whose magnitude is directionally dependent.

Secondly, the divergence or div operator (\cdot) is a dot notation abbreviation

characterized by $div(\mathbf{u}) = \nabla \cdot \mathbf{u} = \frac{\partial u_x}{\partial x} + \frac{\partial u_y}{\partial y} + \frac{\partial u_z}{\partial z}$. The divergence function is only

valid for vector values and produces a scalar quantity [49]. Armed with these

definitions, the previously-mentioned equations may now be explored. The

conservation of mass equation is represented as a material derivative ($\frac{\partial\rho}{\partial t}$) and

relies on the time rate of change in a material particle's density (ρ) within the

three-dimensional space defined by the velocity vector (\mathbf{u}). This constraint

ensures that material is neither created nor destroyed through the process of

combustion. In addition to previously mentioned variables, the species

conservation equation preserves ingredient balance throughout the compartment

by considering volumetric production rate (\dot{m}_i'''), elemental mass fractions (Y_i),

and diffusion coefficient (D). The left portion of the equivalence describes

species accumulation due to density change and species inflow and outflow.

Meanwhile, the right portion counters with species inflow and outflow due to

diffusion and elemental production rates. Conservation of momentum provides a

velocity and pressure coupling to preserve momentum within the fluidic

representation. Momentum-altering affects caused by the environment's vorticity

(ω), viscosity (τ), gravity (\mathbf{g}), and external forces excluding gravity (\mathbf{f}) are

accounted for. Also notice that variations in applicable gravitational forces due to changes in material density and existing particle velocities are represented. The divergence constraint calculates and limits particle flow deviation through the combination of the material derivative, conservation of mass, and conservation of energy terms. The integral term accounts for reaction enthalpy by assuming constant specific heat over the temperature range. The assumption of temperature-independent specific heat only results in the exclusion of minor divergence terms while greatly reducing calculation costs [45]. Lastly, the equation of state establishes an equivalency between background pressure at a given time, $p_0(t)$, and the product of density (ρ), temperature (T), and the universal gas constant (\mathfrak{R}) divided by material mass (M). The low Mach number equations assume that density and temperature are inversely proportional. It should also be recognized that the product of density and volume yields mass ($\rho V = M$). This relation, in conjunction with the equation of state, roughly resolves to the ideal gas law ($PV = n\mathfrak{R}T$), differing only by the number of moles of gas (n). In practice, FDS also uses the equation of state to calculate temperature.

Within the realm of fire simulation, software tools serve as an excellent means of fire hazard analysis. One such program that has been shown, through practical experimentation, to be particularly adept at modeling fire scenarios is NIST's Fire Dynamics Simulator. In conjunction with its visualization counterpart,

Smokeview, FDS can provide tremendous amounts of data and insight. This information may be used to investigate, verify, augment or, in some cases, supplant real-world fire situations and thereby reduce expense and possible loss.

Chapter 4

Investigative Approach

4.1 Overview

With the intent of demonstrating damage potential and exploring aspects of layout and design, the subsequent investigation considers various facets of data center fire hazards. These elements include possible post-fire outcomes and methods of suppression. This exploration is facilitated through the implementation of NIST's Fire Dynamics Simulator (FDS) software package discussed in Chapter 3. Through these simulations, a clearer understanding of data center fire vulnerability can be gleaned.

4.2 Assumptions

Because a fire's inception possesses a single point of origin before spreading, the data center combustion model constructed in this study is simplified to a single rack-mounted computer system. Enhancing the model's flexibility, this evaluation allows for the simulation of behavior and pyrolysis product generation related to a single electronic unit. Additional fuel loads, such as supplementary rack systems or wiring interconnects, may then be considered individually or as targets of preliminary flame propagation. The previous analysis has shown that the first step in any effective computer room fire suppression system is to shunt electrical power to the compartment and disengage ventilation systems.

Therefore, it was unnecessary to model damage incurred by electrical arcing or forced-air draft environments. Finally, to ensure maximum available fuel exposure, the upper surface of the lowest circuit board was selected as the point of ignition. These assumptions help to establish a theoretical worst-case scenario after fire detection.

4.3 Experimental Model

The selected experimental model represents a vertical, rack-mount computer enclosure characteristic of a data center. This particular cabinet contains six individual circuit board tray divisions and is constructed of steel. Paralleling previous small-scale fire tests performed by NIST [50], PMMA is chosen as an adequate representation of a typical printed circuit board fuel load. The data center walls are represented as concrete structures consistent with typical construction.

Both unsuppressed (free burn) and water suppressed simulations are implemented. The factors dictating sprinkler effectiveness are droplet size and distribution, momentum of spray, ceiling clearance, and magnitude of fire [51]. Due to water mist's infancy and implementation variation, an adequate standardized model of a misting sprinkler, including droplet size and distribution, is unavailable. Therefore, for its extended coverage potential, the default Central K-11 sprinkler is implemented within the various suppression tests (Appendix E).

Finally, based on projected methods of extinguishment, an in-cabinet fire suppression system is implemented.

4.4 Parameters

For layout purposes, the FDS coordinate system is based on a three-dimensional Cartesian grid composed of X, Y, and Z axes. The physical enclosure was modeled as a 2.5 m x 3.0 m x 3.0 m (8.20 ft. x 9.84 ft. x 9.84 ft.) area. These dimensions established a compartment space large enough to visualize products of combustion while simultaneously allowing for the observation of radiative and convective effects via boundary conditions. The steel rack-mount cabinet was centered in the room and measured 0.7 m x 0.6 m x 2.0 m (2.30 ft. x 1.97 ft. x 6.56 ft.). Each of the six circuit boards was 0.6 m x 0.6 m x 0.005 m (23.62 in. x 23.62 in. x 0.20 in.) in dimension. Thermocouples were placed 10 cm (3.94 in.) in front of each circuit board. Both circuit boards and thermocouples were labeled from one through six beginning with those at the lowest Z-axis value. To ensure adequate fidelity, a 50 cell x 60 cell x 120 cell computational grid was established. This resulted in an array of 360,000 cells measuring 5 cm x 5 cm x 2.5 cm (1.97 inches x 1.97 inches x 0.98 inches). As a side note, these specifications resulted in average processing times of one to almost three weeks on a 2.8 GHz Pentium 4 equivalent machine with 1 Gigabyte of memory. The prescribed layout is shown in Figure 4.4.1.

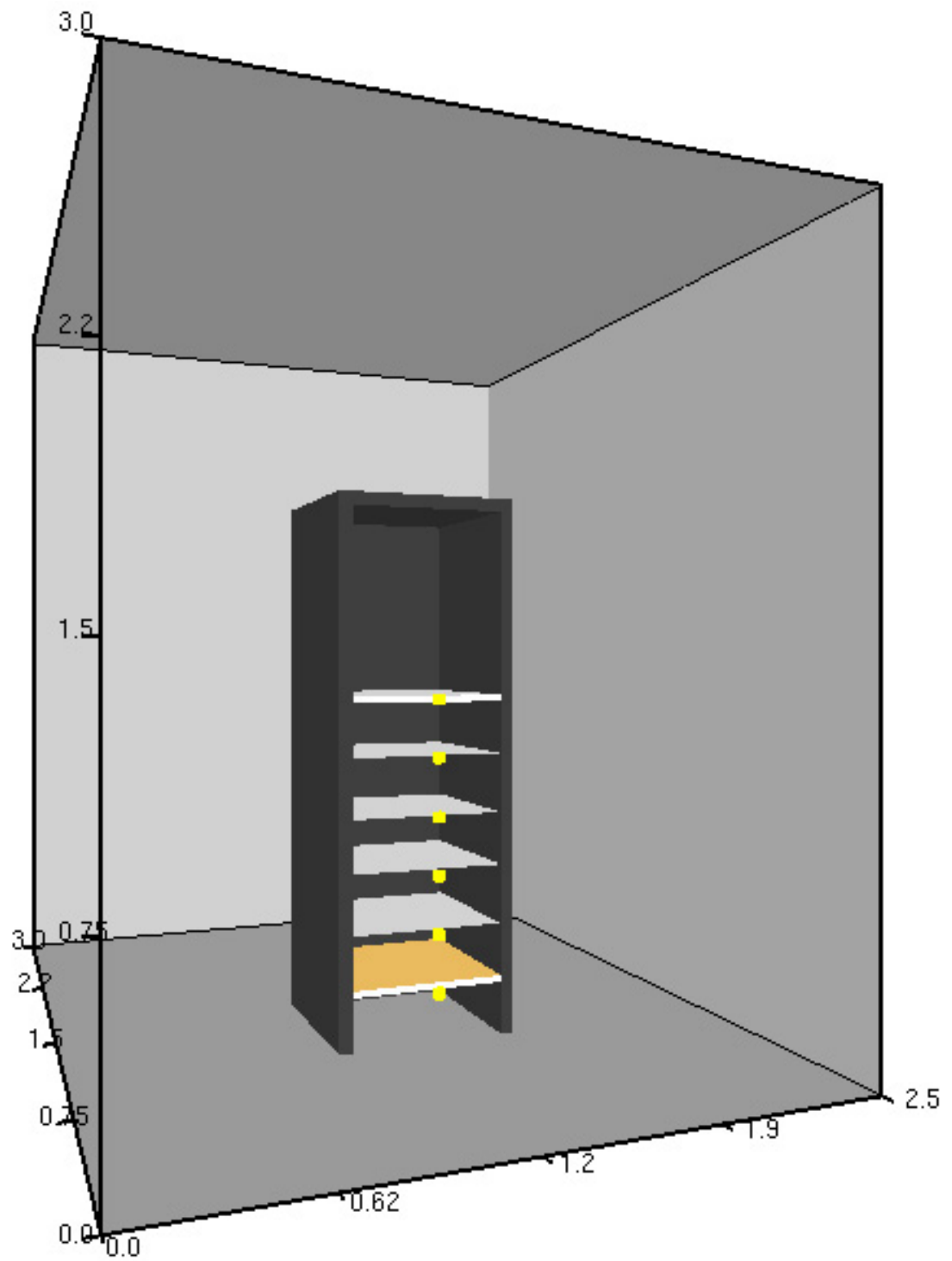


Figure 4.4.1. Compartment Design

Based on previous analysis, telecommunication facility fires typically commence with 5-10 kW potentials [52]. In comparison, small trash can fires may generate heat release rates of more than 15 kW [53] and typically reach rates of 100 kW. Therefore, a worst-case-scenario heat release rate of 10 kW was initially selected and expanded upon. For comparative purposes, fires were defined in two manners. The first method implemented FDS's vent syntax and established a fire over a portion of a circuit board. Subsequent tests employed FDS's surface syntax to define a broader site of combustion that covered the entire upper surface of a circuit board. Suppressed and unsuppressed tests were performed under each scheme. A summary of the set of experimental fire simulations is contained in Table 4.4.1. Within this table, suppression posture is defined by the sprinkler's physical location within the cabinet followed by its spray orientation. Therefore, a designation of "back aimed forward" may be read such that a sprinkler was positioned at the rear of the cabinet and aimed outward (parallel to the compartment floor) toward the thermocouples. Due to cabinet symmetry, sprinklers placed on the right side and aimed left could just as easily be interpreted as being placed on the left side and aimed right. However, as computer cabinets are typically arranged side-by-side in rows, data center layouts are more accommodating of rear-mounted fire suppression systems. Hence, a larger number of simulations operated under that methodology.

Table 4.4.1. Set of Experimental Fire Simulations

Containment Presence / Posture	Fire Type	Heat Release Rate
Unsuppressed	Vent	10 kW
Unsuppressed	Surface	10 kW
Unsuppressed	Surface	1,296 kW
Suppressed (K-11 Back aimed forward)	Vent	10 kW
Suppressed (K-11 Back aimed forward)	Vent	1,296 kW
Suppressed (K-11 Back aimed forward)	Surface	10 kW
Suppressed (K-11 Back aimed forward)	Surface	1,296 kW
Suppressed (K-11 Back aimed downward)	Vent	10 kW
Suppressed (K-11 Back aimed left)	Vent	10 kW
Suppressed (K-11 Right aimed left)	Vent	10 kW
Suppressed (K-11 Right aimed left)	Surface	1,296 kW

As a method to dictate fire potential, FDS draws on its Heat Release Rate Per Unit Area (HRRPUA) keyword designation. Fire vent dimensions of 0.05 m x 0.05 m established a HRRPUA of 4,000 kW/m² (4,000 kW/m² x 0.0025 m² = 10 kW). In surface tests, the upper surface of the lowest circuit board was defined as the source of combustion. This established a 0.6 m by 0.6 m surface area which necessitated a HRRPUA value of 28 kW/m² (28 kW/m² x 0.36 m² = 10 kW). In an effort to investigate the impact of a large-fire, further testing investigated greater heat release rates. Within the fire protection arena, a heat release rate of 1,000 kW is commonly accepted as a small-room flashover threshold. In some cases, slightly higher values may be reported. Therefore, large-fire impacts were explored by observing fires possessing heat release rates of nearly 1,300 kW (3,600 kW/m² x 0.36 m² = 1,296 kW). Paralleling this discussion, sample FDS input file listings are contained in Appendix F.

Although an infinite number of simulation combinations exists, this particular set of experiments examined key aspects of simulated fire type, presence or absence of containment, and proposed minimum and maximum heat release rate values. Adjustments in suppression orientation and placement accounted for the largest parameter variance, followed by fire type and size. These trials reinforced the need for future investigation and innovation.

Chapter 5

Results

5.1 Overview

Variations in fire size (small or large), combustion type (vent or surface), suppression availability (present or absent), and suppression posture (location and orientation) allowed for the construction of numerous fire scenarios. In all, various aspects of eleven independent simulations were explored. However, acknowledging and appreciating the development of common themes and trends, the following analysis focuses on unsuppressed and suppressed versions of the more representative FDS vent-style fire.

5.2 Thermal Effects

Thermal effects were observed and measured via a number of methods including isosurface, various slice files, boundary measurements, and a six-node thermocouple tree. Isosurfaces provided tangible representations of fire flow and flame impingement. Although extracted from an unsuppressed fire simulation, the isosurface example shown in Figure 5.2.1 represents initial fire spread common to both suppressed and unsuppressed scenarios. It illustrates direct flame impingement on circuit boards one and two. Low heat release rate scenarios demonstrated significant flame contact to circuit boards one, two, and three. Meanwhile, large heat release rate scenarios revealed flames washing

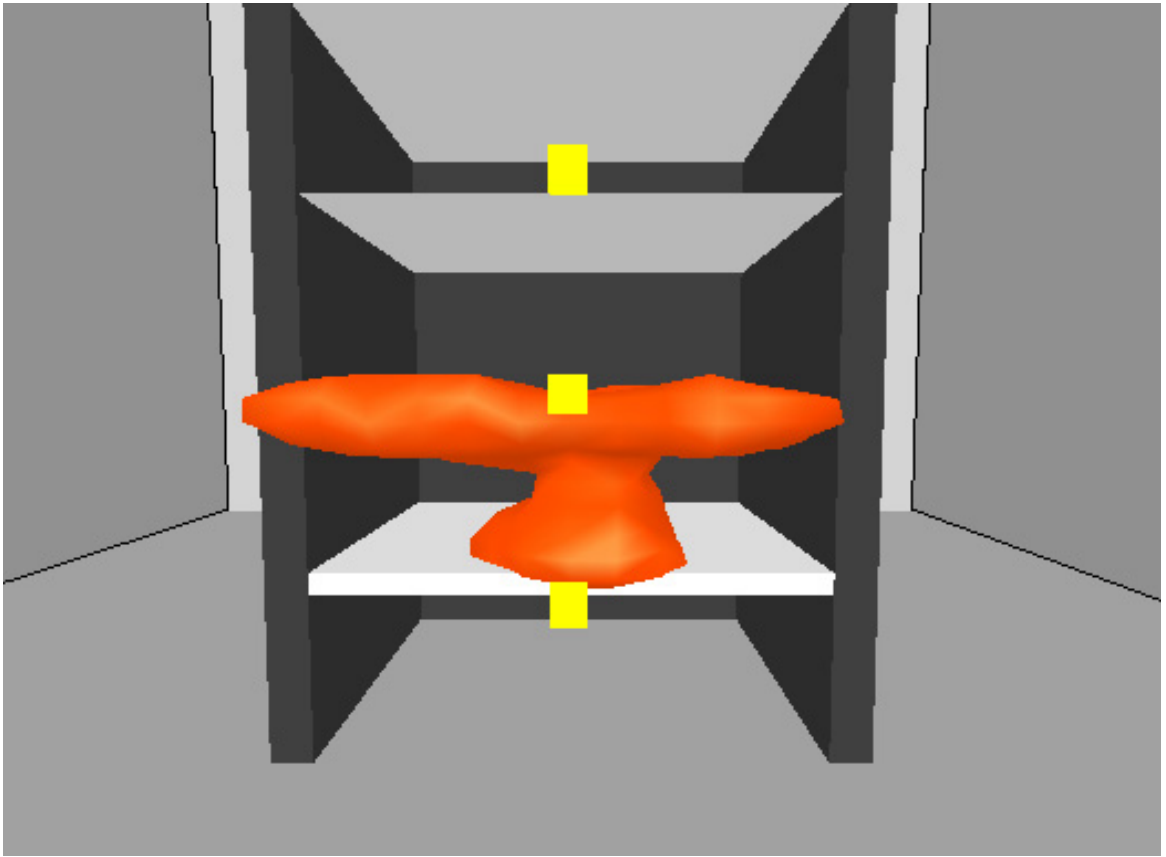


Figure 5.2.1. Isosurface Example

over all six circuit boards. These types of sustained fire contact typically spell disaster for the functionality of components in question.

Slice files, both normal and vector, assisted in the measurement of fire properties and gaseous flow and entrainment. The examples in Figure 5.2.2 are representative of slice file appearance and implementation. Within the sphere of thermal effects, normal slice files captured and displayed the continuous temperature gradient and heat concentrations as combustion progressed. Vector slices captured these elements as well. However, they also provided directional heat flow and intensity and gaseous entrainment insight. Allowing more flexibility in placement, slice file data corroborated the abovementioned damage assessment and provided numeric temperature readings as support.

Boundary file options provided further insight into potential thermal damage. By recording surface thermal properties, boundary files illustrated destructive potential to the computer cabinet via temperature, radiative flux, and conductive flux measurements. Because these measurements are not only restricted to the computer cabinet, but are also captured for the compartment's walls, prospective damage for additional fire targets may be assessed as shown in Figure 5.2.3. Once again, using boundary file surface temperature measurements, both circuit board and computer cabinet damage was observed. Figure 5.2.4 represents peak combustion surface temperatures for the unsuppressed, small heat release

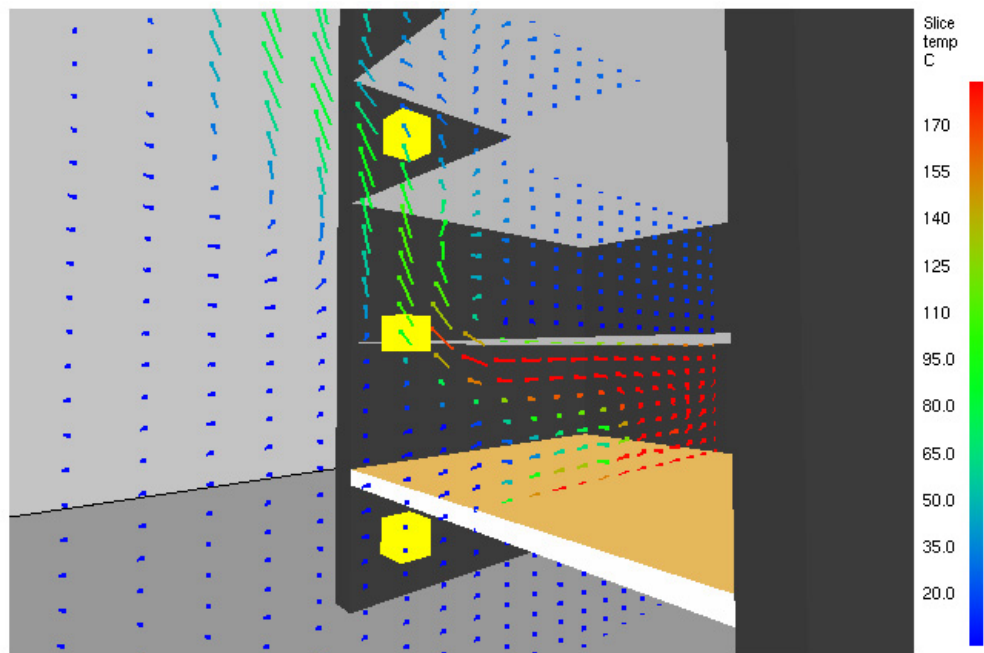
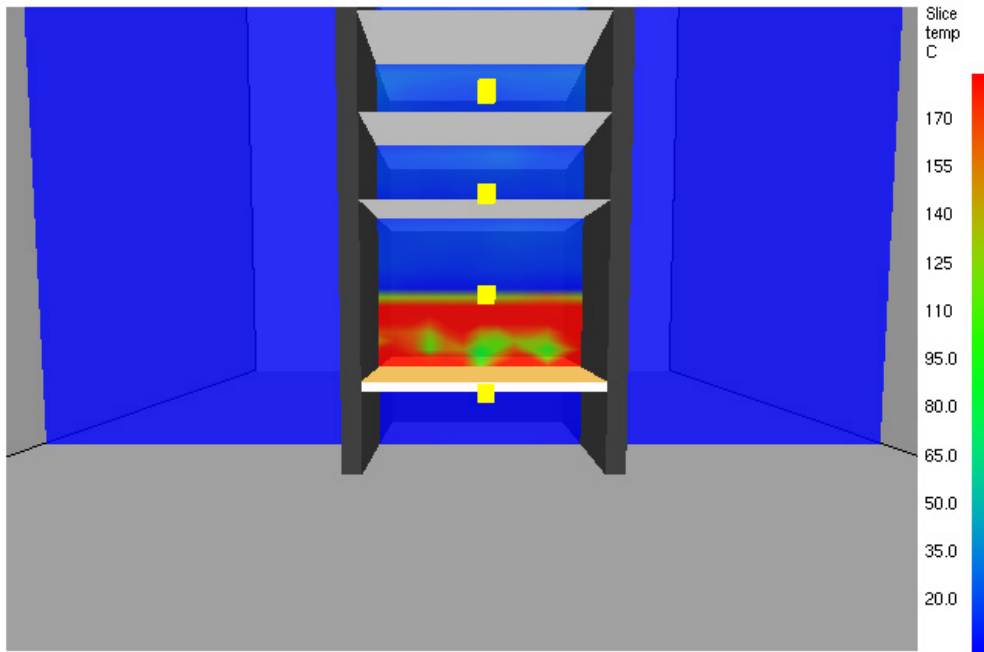


Figure 5.2.2. Slice File Examples (Normal and Vector)

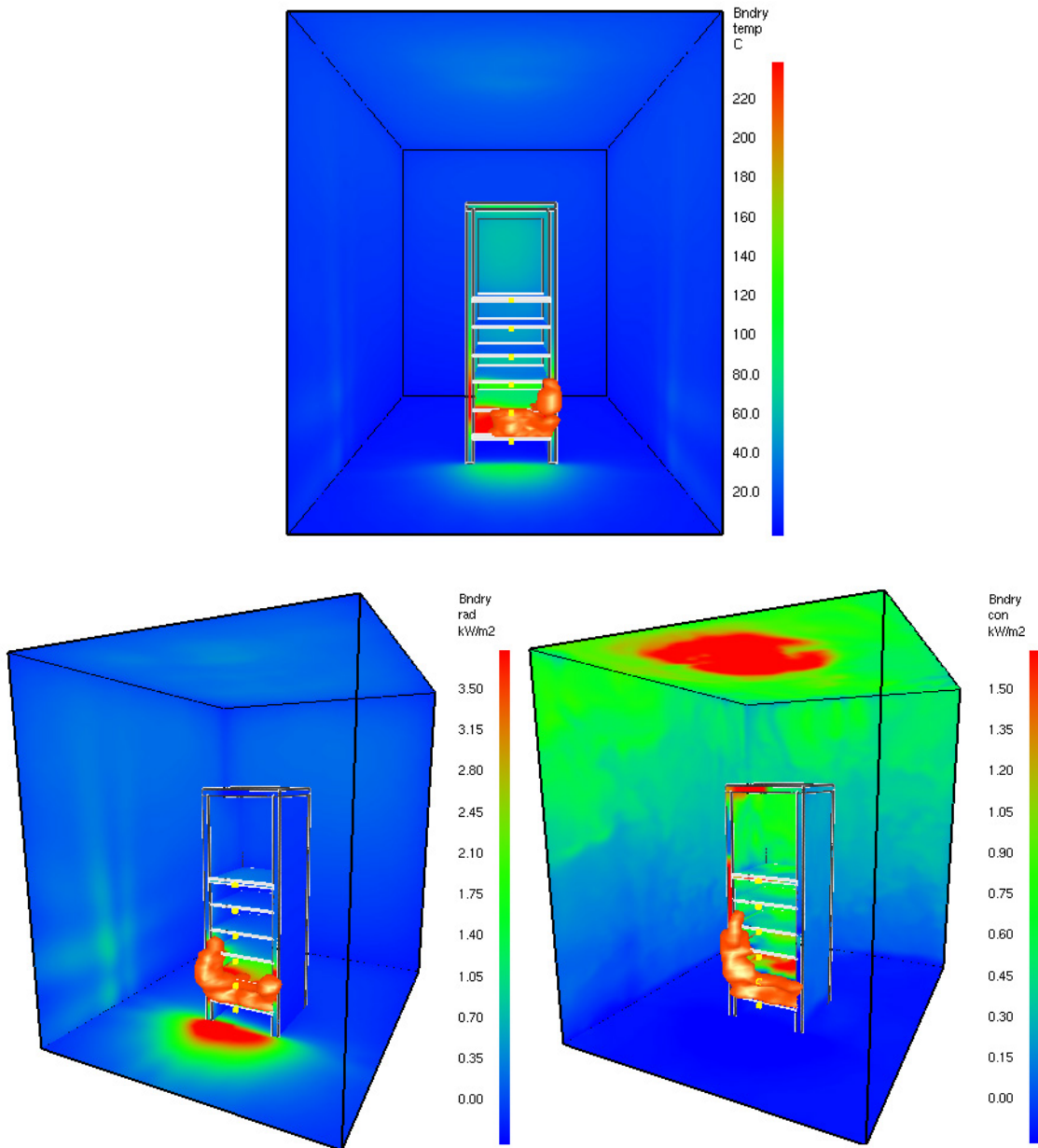


Figure 5.2.3. Boundary File Examples (Temperature, Radiative Flux, and Convective Flux)

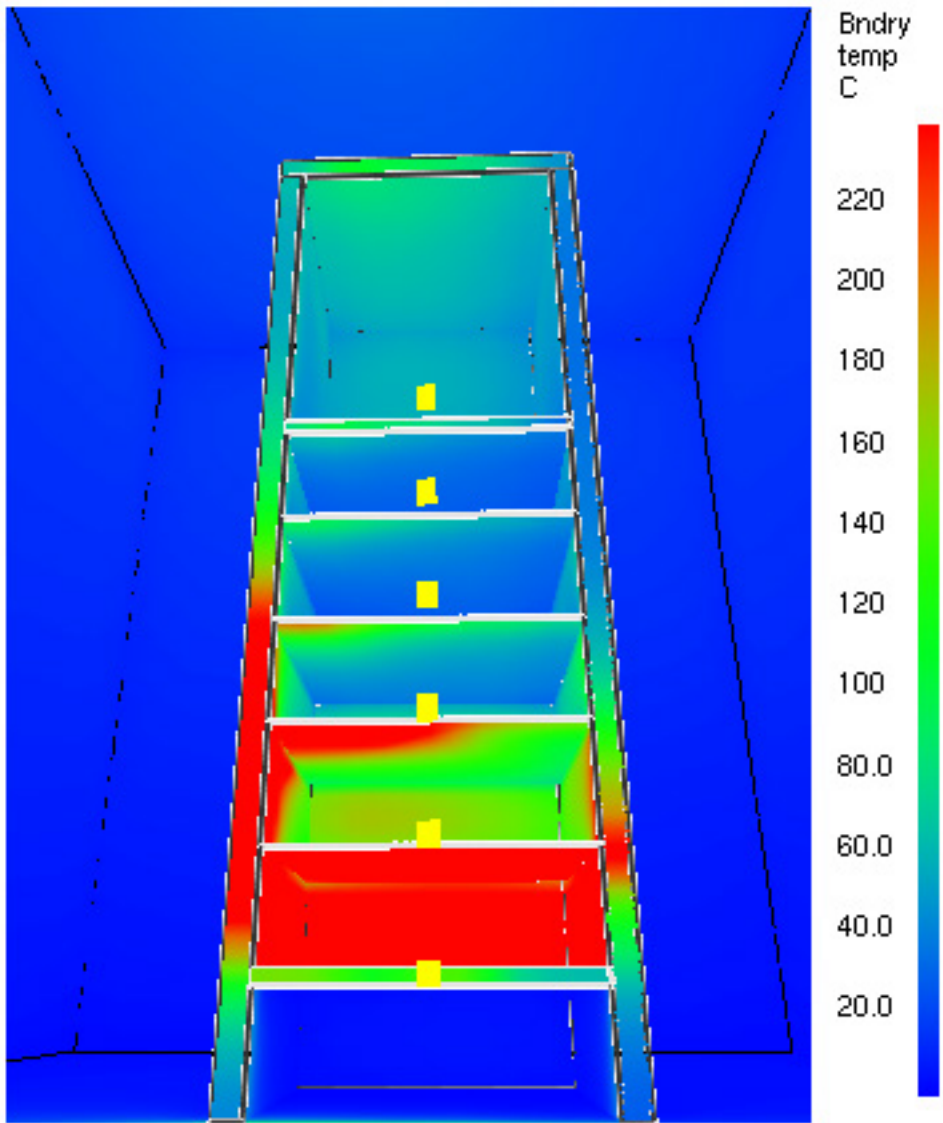


Figure 5.2.4. Boundary Temperature Measurements (Small HRR)

rate fire. Similarly, Figure 5.2.5 displays the same measurements for the unsuppressed, large heat release rate scenario. Accepting NFPA's relatively forgiving functional computer equipment thermal threshold of 79.4°C, even in the smaller fire scenarios, it should be noted that excessive and damaging temperatures were inflicted on all circuit boards.

Represented as the yellow boxes in front of each circuit board, thermocouples imparted a further means of evaluating thermal conditions. Figure 5.2.6 shows numeric temperature measurements taken over time during the unsuppressed burn with small heat release rate. The thermocouples registered peak values after approximately 250 seconds of combustion with the highest readings occurring at levels above the site of ignition. Specifically, thermocouples 3 and 4 registered values approaching 650°C (1,202°F). Additional heat-related simulation aspects, Figures 5.2.7 through 5.2.11, are represented below. As additional material became involved, heat release rates of over 130 kW were observed. Radiative loss levels climbed slightly higher than 75 kW. Convective gains barely topped 1.30 kW. Lastly, heat loss due to conduction peaked at slightly more than 30 kW. Although various scales are denoted, these thermal-property figures all possess near-peak values that are coincident with the fire's maximum burn rate. As the fuel supply was depleted, the fire's size diminished and values declined and began to return to pre-blaze conditions.

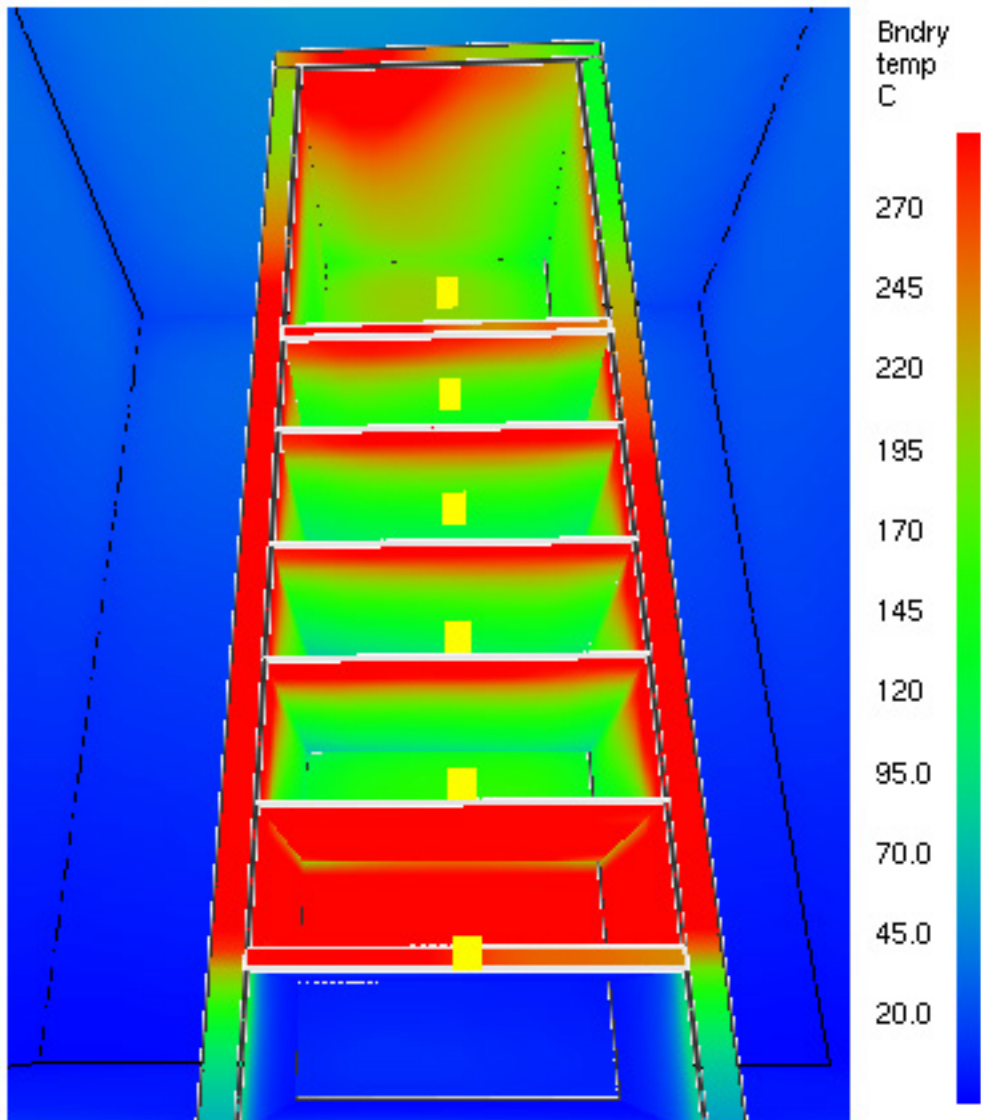


Figure 5.2.5. Boundary Temperature Measurements (Large HRR)

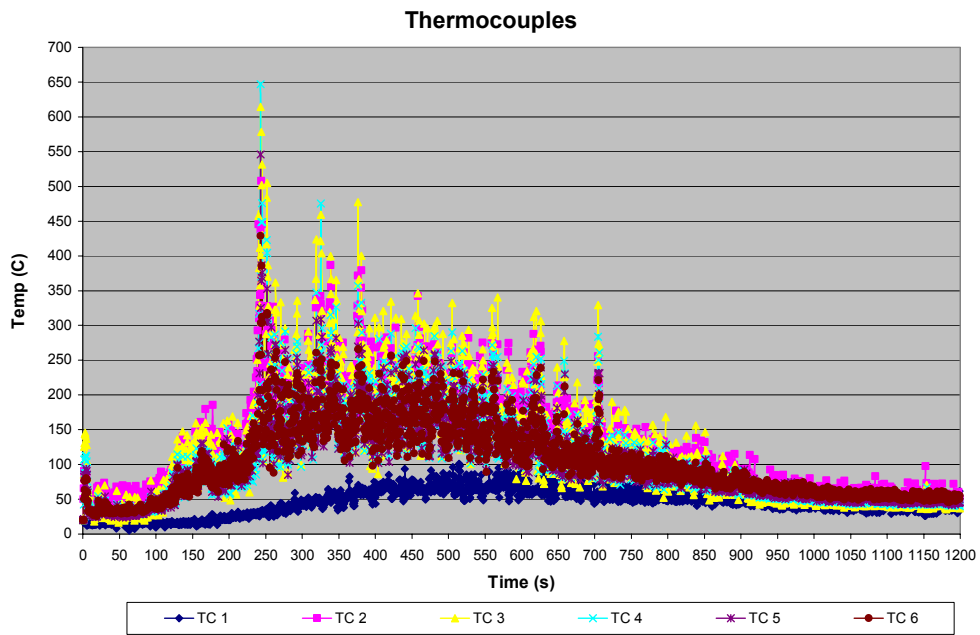


Figure 5.2.6. Thermocouple Plot

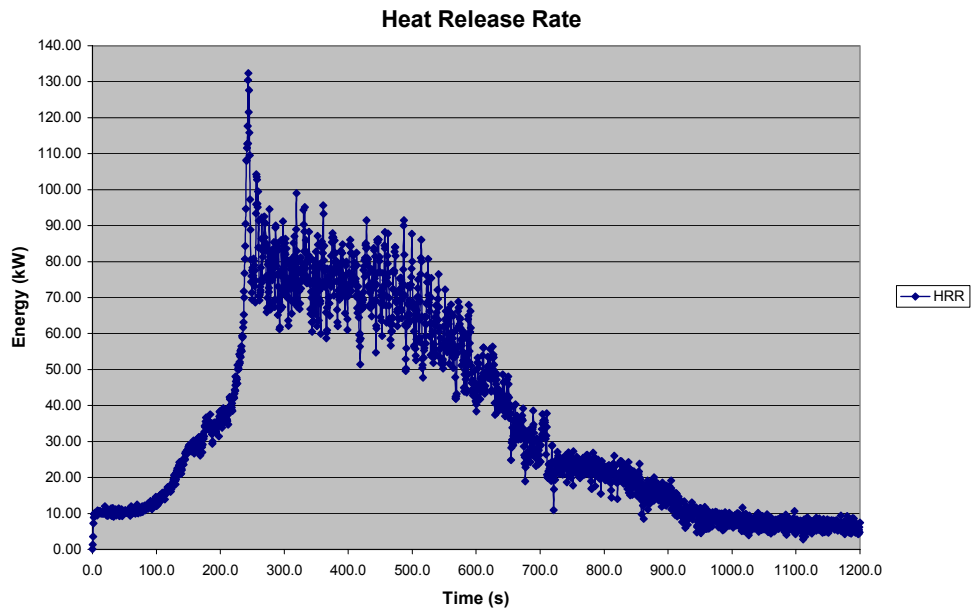


Figure 5.2.7. Heat Release Rate Plot

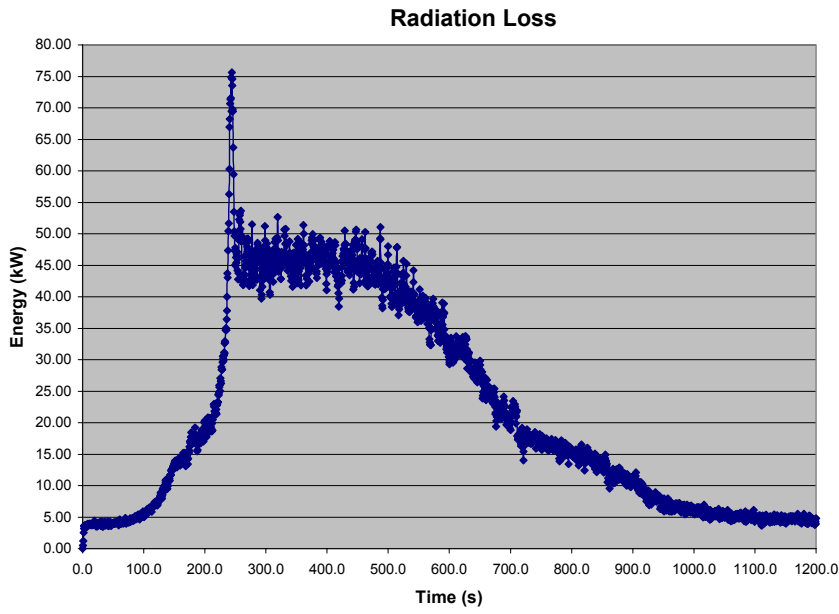


Figure 5.2.8. Radiation Loss Plot

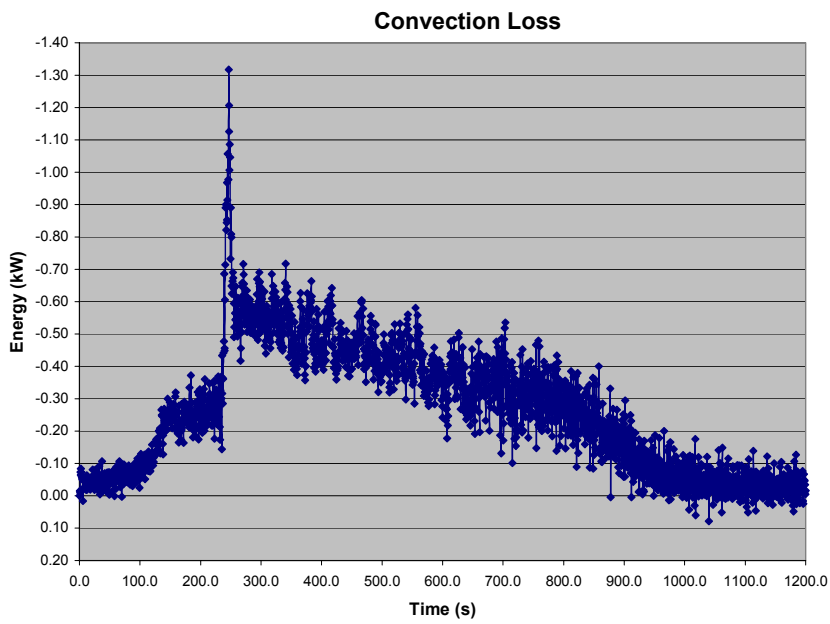


Figure 5.2.9. Convection Loss Plot

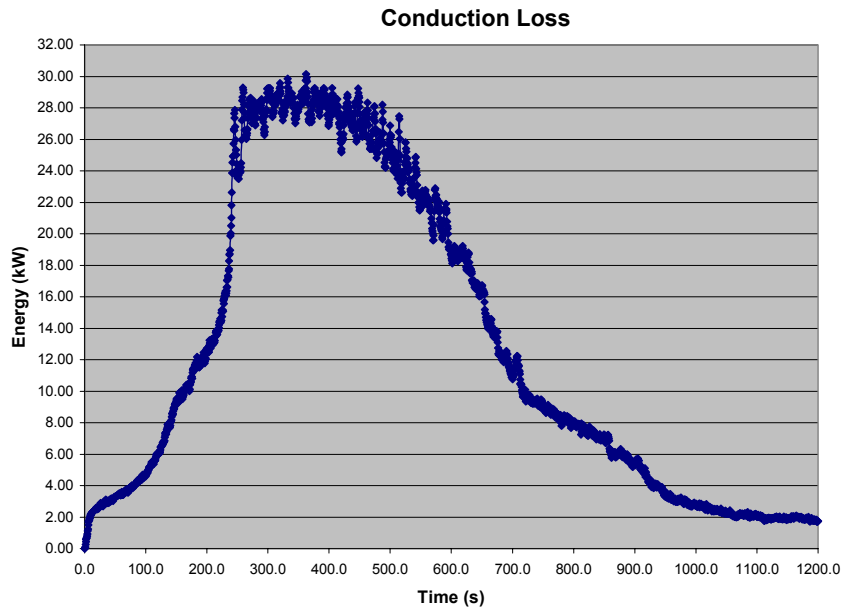


Figure 5.2.10. Conduction Loss Plot

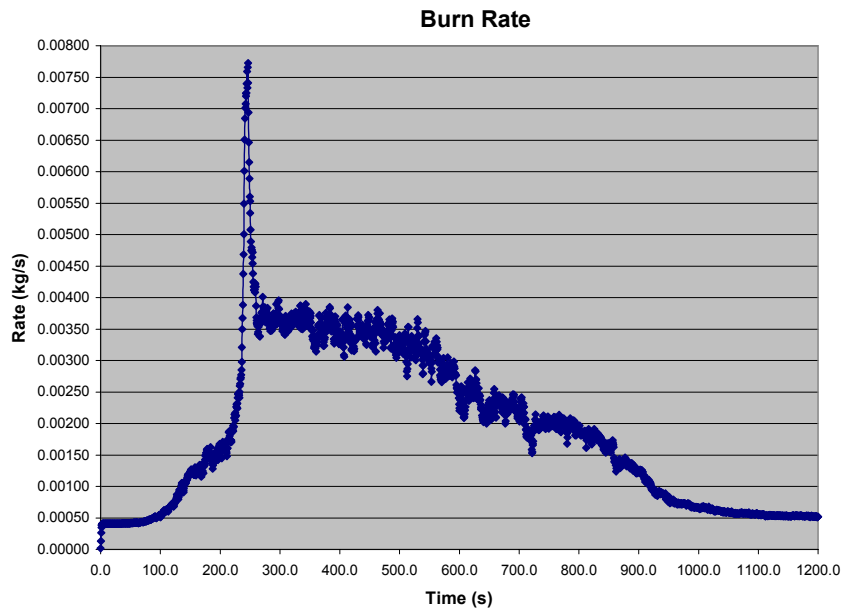


Figure 5.2.11. Burn Rate Plot

Although explicit times and quantitative measurements were initially unknown, these types of results were anticipated and are consistent with general fire experience. In large-fire simulations, flame intensity grew dramatically and combustion rates multiplied. Similar tests involving telecommunication switch gear bays showed thermocouples reaching peak values in approximately 10-12 minutes and flames leaping to heights of 2-4 meters (6.56-13.12 feet) above a cabinet [39]. Before burning out, analogous results were recreated via the unsuppressed, large heat release rate simulation with the result of direct flame impingement on the compartment ceiling, as shown in Figure 5.2.12.

Simulations involving standard sprinkler suppression emphasized water-misting-literature findings and produced a mixed outcome. As shown in Figure 5.2.13, although the course-spray, K-11 sprinkler was successful in drastically reducing combustion and cleansing the cabinet's interior of fire products, its low-density spray and large droplets were not reliably able to entirely extinguish the fire after activation. In this figure, inactive and active sprinklers are represented by red and green blocks, respectively. Upon sprinkler activation, water simultaneously worked to contain the fire and force it out of the enclosure. Although the fire was not always extinguished, it should be noted that the presence of fire suppression yielded appreciable results, as shown by the suppressed thermocouple plot in Figure 5.2.14. While the temperature spike occurred at approximately the same point in time as the unsuppressed example, its peak values were lower and fell

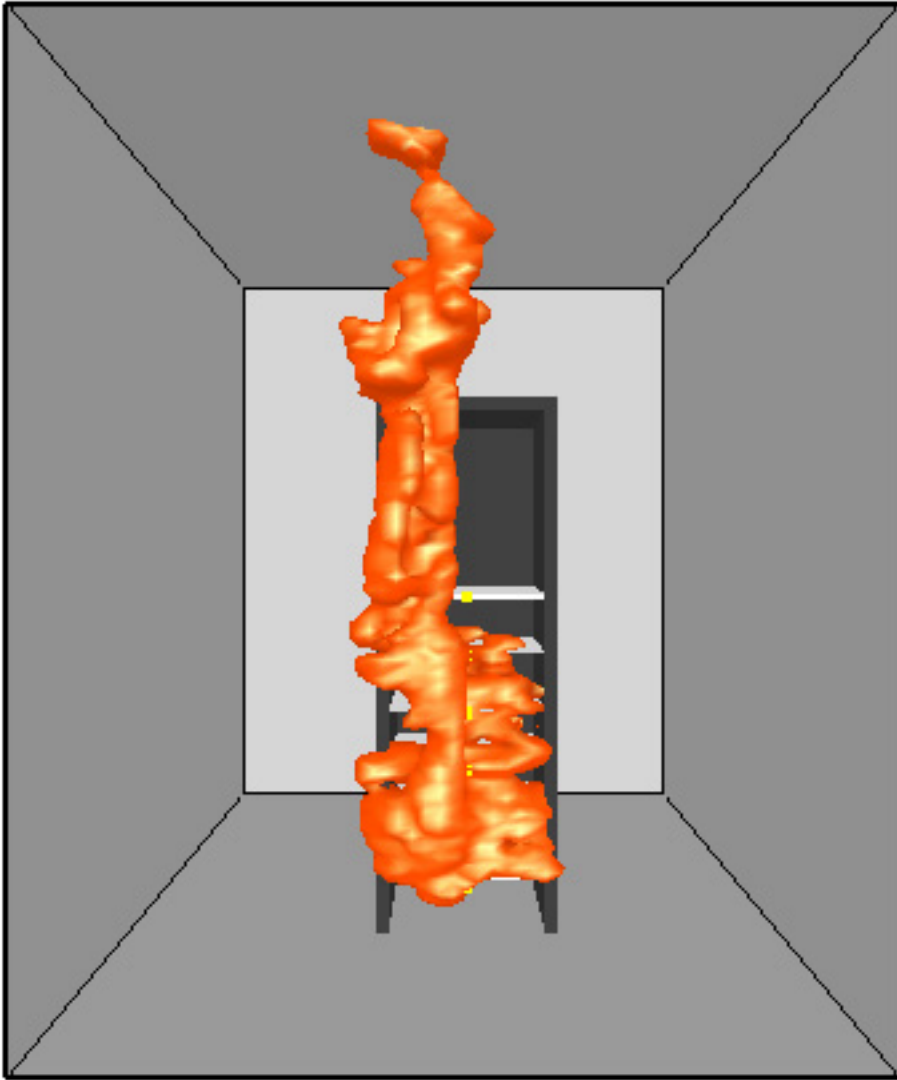


Figure 5.2.12. Ceiling Flame Impingement

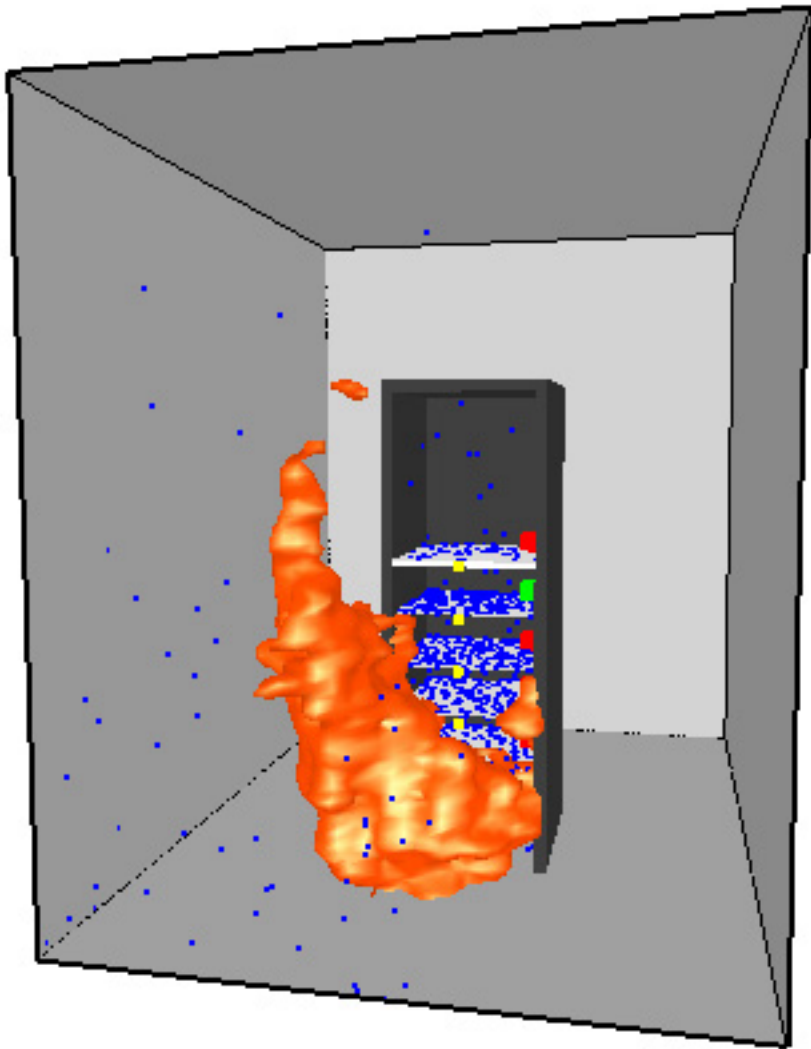


Figure 5.2.13. Sprinkler Activation and Suppression

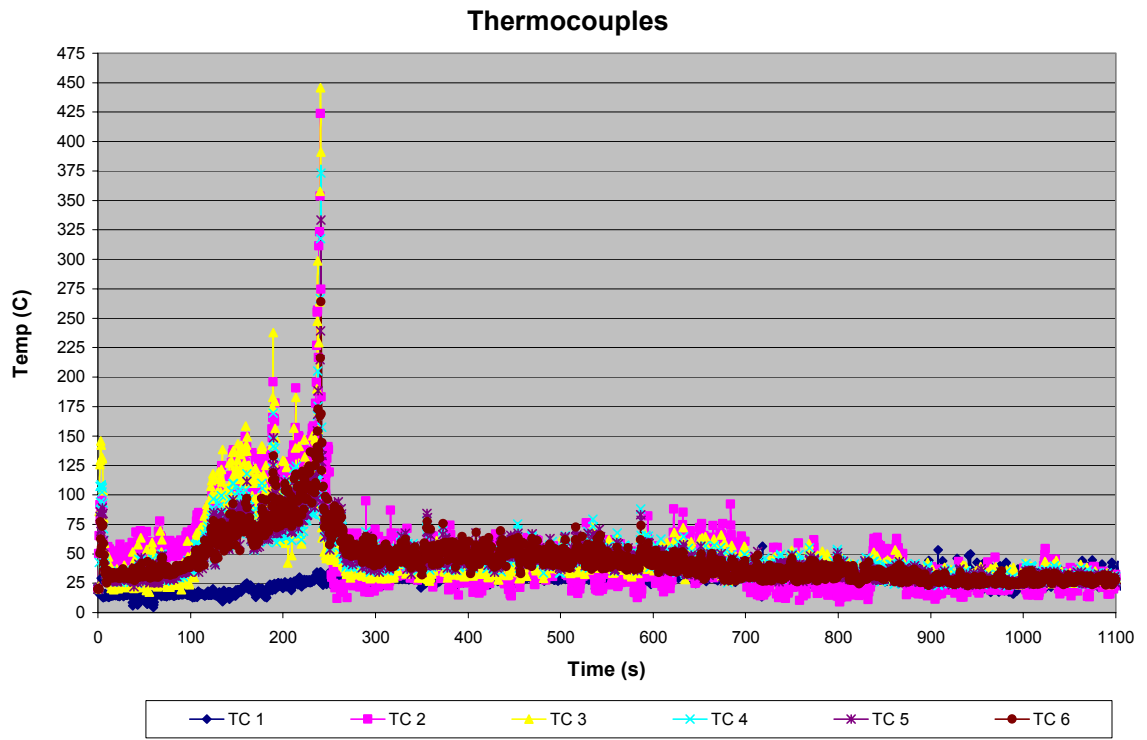


Figure 5.2.14. Suppressed Thermocouple Plot

off rapidly as the sprinklers doused the cabinet with water. Except for thermocouples located in the fire's immediate vicinity, temperatures quickly fell to below 75°C. These results confirmed water-based sprinkler effectiveness and demonstrated excellent potential for component protection.

5.3 Mixture Fraction

Similar to the HRR isosurface, FDS's mixture fraction isosurface allowed for direct visualization of fire and smoke production and integration. Seen both emblematically through isosurface (Figure 5.3.1) and fluidically via slice file (Figure 5.3.2), the mixture fraction representation exhibited toxic gas flow patterns, illustrated key areas of impact, and identified sites of increased corrosive damage. As shown in Figure 5.3.1, the mixture fraction isosurface denoted flame and smoke separation in an observable, yet visually-obstructive manner. However, the partial transparency of a mixture fraction slice file allowed for greater visualization of flame and smoke separation and flow.

5.4 Species

A final source of data produced by FDS was that of species production. Species results modeled classic trends. As the fire burned on, fuel and oxygen levels decreased. Meanwhile, soot, water, and toxic/corrosive gas levels increased. In particular, carbon dioxide (CO₂), as its levels climbed almost 4 kg, and nitrogen (N₂), augmented by nearly 2 kg, amounts experienced the largest

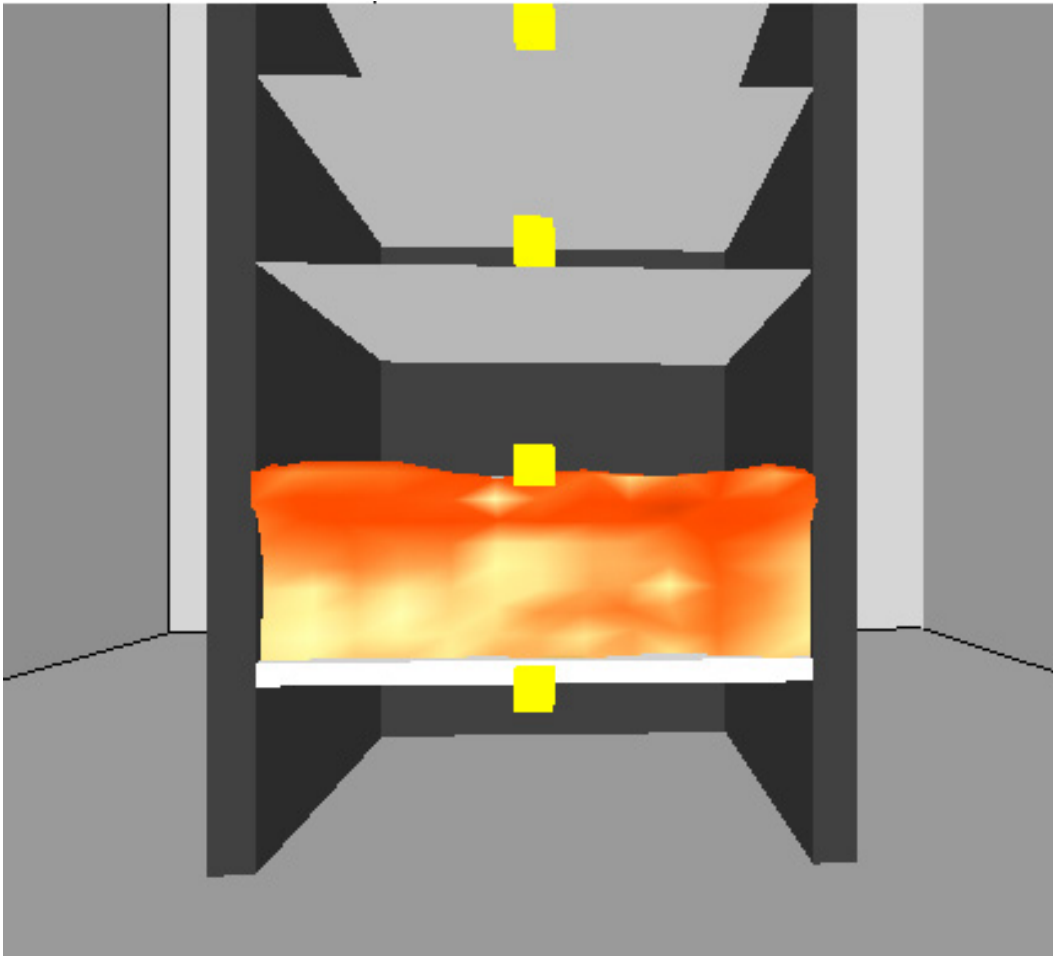


Figure 5.3.1. Isosurface Mixture Fraction

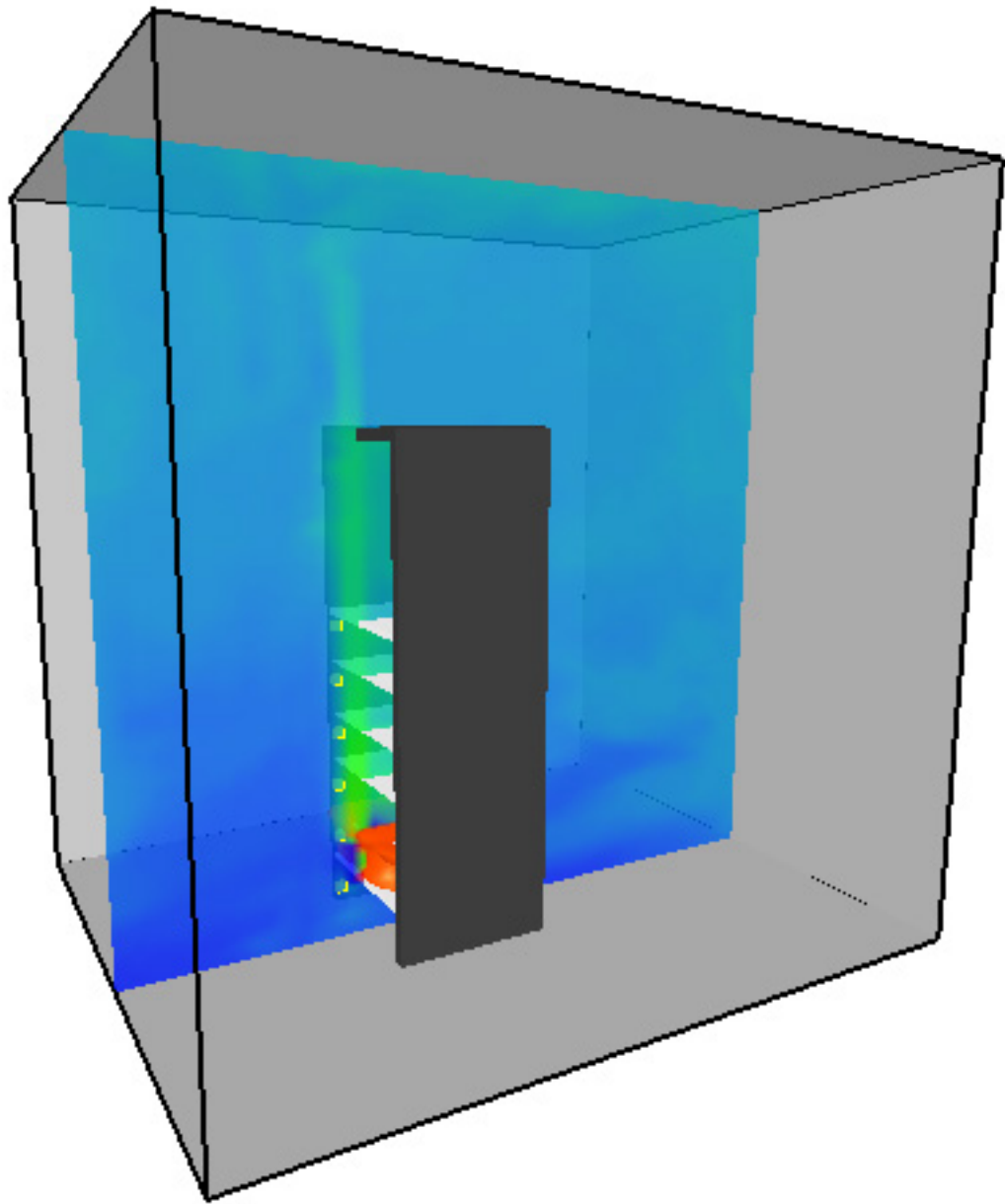


Figure 5.3.2. Slice File Mixture Fraction

increases. Although the compartment's initial oxygen supply decreased greatly, large amounts of water vapor were formed. As the water vapor and the nitrogen content of the fire's byproducts combined, it should be noted that corrosive nitrous and nitric acids were formed and deposited.

Because species data was generated for the overall fire compartment, localized deposition of corrosive agents and soot could not be accurately determined. One possible method of estimation would be to assume a uniform byproduct distribution throughout the fire compartment. Under this premise, individual mass increases could be divided by the number of computational grid cells. Continuing this line of thought, area-specific deposition amounts could be determined by calculating the number of grid cells intersected by the target in question. For example, in the data presented within Figure 5.4.1, nitrogen levels increased by 1.42 kg ($1.42 \times 10^9 \mu\text{g}$). The simulation grid was designed to have 360,000 computational cells measuring 5 cm in width and length. Each circuit board in the simulation measured 60 cm in width and length. Consequently, the upper surface of a single circuit board would intersect 144 cells. Therefore, quick division ($1.42 \times 10^9 \mu\text{g} / 360,000$) yields an approximate concentration of 3,944 μg per cell. With 144 affected cells ($5.68 \times 10^5 \mu\text{g}$) spanning 3,600 cm^2 , additional calculation ($5.68 \times 10^5 \mu\text{g} / 3,600 \text{cm}^2$) equates to contamination levels of 157.8 $\mu\text{g}/\text{cm}^2$. Unfortunately, as it has been previously established, soot and corrosive byproducts are not homogeneously distributed throughout an

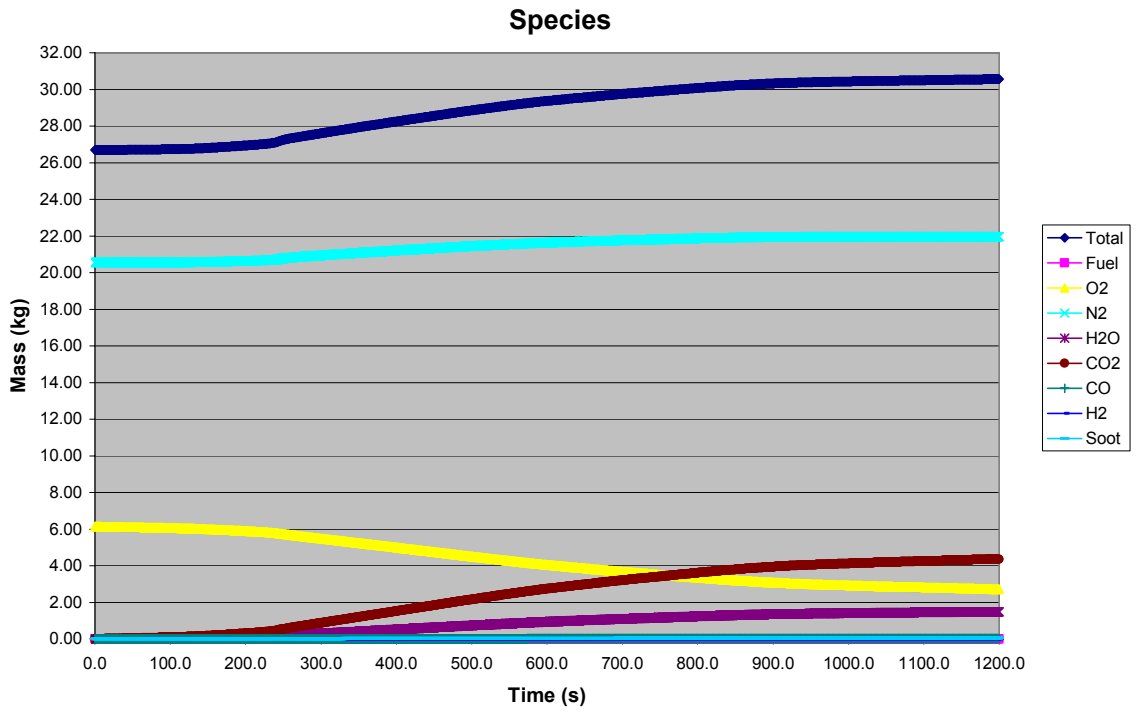


Figure 5.4.1. Species Plot

atmosphere of combustion. Hence, an assumption of uniformity would yield inaccurate results.

As these results have shown, thermal effects, mixture fraction, and species production each play a pivotal role in fire outcomes. Fortunately, or unfortunately as the case may be, it was discovered that the fire's thermal effects dominated the verdict of component tenability. These results proffered valuable information related to data center fires and equipment survival.

Chapter 6

Conclusions and Future Work

6.1 Recommendations

Although by no means comprehensive, this work serves as a catalyst to further research in the field of computer fire modeling. The use of computer-based simulation tools provides a valuable avenue of insight and protection. Through scenario modeling, several fire effects and suppression techniques may be explored that would otherwise prove to be too costly or impractical. It has been shown that computer data centers pose a vulnerability to the effects of fire—especially thermal aspects. It became readily apparent that even relatively small fires common to this venue have disastrous potential. Given the level of importance surrounding data and equipment in computing environments, this liability may be quite significant. Water-based suppression tests yielded some self-evident results. Those being, sprinklers are more effective when positioned closer to and oriented toward the source of combustion. Although standard sprinkler equipment proved to be helpful, further exploration of hybridized gas-water and water mist suppression techniques is also merited. Obvious areas of future exploration include full-scale, real-life test burns and additional simulation. The value of future investigative results may also be enhanced by the inclusion of modeled detection systems.

As referenced in the FDS User's Guide, simulations and calculations are based on an evolving fire model and, given the correct conditions, can be accurate to within 10%-20% [45]. The complexity involved in fire modeling mandates an understanding of implied assumptions and technological limitations. As investigation continues to reveal new insights, FDS's computational fluid dynamics model can be updated. However, in the analysis of this scenario, the simulation provided findings that were consistent with anticipated outcomes.

References

- [1] European Flame Retardants Association, "Reducing the Risk of Fire: Fire Statistics," vol. 2004. Brussels, Belgium.
- [2] "Annual Report 2000," Council of Canadian Fire Marshals and Fire Commissioners, 2000.
- [3] National Fire Protection Association, "NFPA Fact Sheets: Electrical Safety."
- [4] United States Department of Energy, *DOE Handbook: Fire Protection*, vol. 2. Washington: United States Department of Energy, 1996.
- [5] A. Hiles, "Computer Fire Risks," *Computers & Security*, vol. 10, pp. 299-302, 1991.
- [6] R. L. Taylor, "LEAD-ACID BATTERIES IN BUILDINGS," Morning Star Industries, Incorporated, 2002.
- [7] "Computer Room Fire - A Computer System Manager's Nightmare." Wellington, New Zealand: The Treasury, 1995.
- [8] "U.S. Army Communications-Electronics Command (CECOM)," 1997.
- [9] M. Wuthrich, "Fire in Zurich -- Hottingen Telephone Exchange -- Chemical Problems," *Technische Mitteilungen PTT*, vol. 12, pp. 536-547, 1970.
- [10] D. O. Manning, "First Interstate Bank Fire," Los Angeles Fire Department Historical Archive, 1999.
- [11] B. Menkus, "Computer-Related Fire Problems Revisited," *Computers & Security*, vol. 8, pp. 581-6, 1989.
- [12] D. M. Karydas, "A Probabilistic Methodology for the Fire Smoke Hazard Analysis of Electronic Equipment," in *Industrial Engineering*. Boston: Northeastern University, 1990.
- [13] "Computing Services," Climate Diagnostics Center, 2004.
- [14] National Fire Protection Association, *NFPA 75: Standard for the Protection of Electronic Computer/Data Processing Equipment*, 1999 ed. Quincy: National Fire Protection Association, 1999.
- [15] M. R. Pallavicini, "Ozone Depletion and Halon: Alternatives For Computer Fire Protection," *EDPACS*, vol. 19, pp. 1-7, 1991.
- [16] Factory Mutual Research Corporation, "A Methodology for Telephone Central Office Fire and Smoke Protection Guidelines." Norwood, MA, 1993.
- [17] C. L. Ford, "Halon 1301 Computer Fire Test Program," Interim Report on Work done by the Ansul Company, Cardox, a Division of Chemetron Corporation, E.I. DuPont de Nemours & Co., Inc., and Fenwal, Inc. Jan 10, 1972.
- [18] F. L. Laque, and Copson, H.R. (ed.), *Corrosion Resistance of Metals and Alloys*. New York: Reinhold Publishing Corporation, 1963.
- [19] M. G. Fontana, *Corrosion Engineering*. New York: McGraw-Hill Book Company, 1986.
- [20] H. Sandmann, and Widmer, G., "The Corrosiveness of Fluoride-containing Fire Gases on Selected Steels," *Fire and Materials*, vol. 10, pp. 11-19, 1986.

- [21] B. S. Skerry, Johnson, J.B., and Wood, G.C., "Corrosion in Smoke, Hydrocarbon and SO₂ Polluted Atmospheres--I. General Behavior of Iron," *Corrosion Science*, vol. 28, pp. 657-695, 1988.
- [22] L. Clerbois, Heitz, E., Ijsseling, F.P., Rowlands, J.C., and Simpson, J.P., "Principles for Scaling of Corrosion Tests," *Br. Corros. J.*, vol. 20, 1985.
- [23] F. M. Galloway, and Hirschler, M.M., "Model for the Mass Transfer and Decay of Hydrogen Chloride in a Fire Scenario," in *Mathematical Modeling of Fires, STP 983*. Philadelphia: American Society for Testing and Materials, 1987, pp. 35-57.
- [24] F. M. Galloway, Hirschler, M.M., and Smith, G.F., "Surface Parameters from Small-scale Experiments used for Measuring HCl Transport and Decay in Fire Atmospheres," *Fire and Materials*, vol. 15, pp. 181-189, 1991.
- [25] B. T. Reagor, "Smoke Corrosivity: Generation, Impact, Detection, and Protection," *Journal of Fire Science*, vol. 10, 1992.
- [26] J. A. M. Gibbons, and Stevens, G.C., "Limiting the Corrosion Hazard from Electrical Cables Involved in Fires," *Fire Safety Journal*, vol. 15, pp. 183-190, 1989.
- [27] A. F. Grand, "Evaluation of the Corrosivity of Smoke from Fire Retarded Products," *Journal of Fire Science*, vol. 9, pp. 44-58, 1991.
- [28] F. M. Galloway, and Hirschler, M.M., "A Model for the Spontaneous Removal of Airborne Hydrogen Chloride by Common Surfaces," *Fire Safety Journal*, vol. 14, pp. 251-268, 1989.
- [29] K. Greenough, "Ph.D. of Restoration Technologies Inc.," 1993.
- [30] I. a. C. P. Beale, "Water Versus Halon 1301: Current Fire Protection Alternatives for Computer Rooms," *EDPACS*, vol. 17, pp. 1-6, 1990.
- [31] D. Butler: I/O Magnetics, 1993.
- [32] B. J. Price, "Computer Room Fire Protection," *Library Hi-Tech*, vol. 8(1), pp. 43-56, 1990.
- [33] Y. Bentor, "Chemical Elements.com," 2003.
- [34] Chemsoc: Royal Society of Chemistry, 2004.
- [35] "The Free Dictionary.com." Huntingdon Valley, PA: Farlex, Inc., 2003.
- [36] J. Williams, "Detect, Spray Computer-Room Fire in 5 Sec," *Electrical World*, vol. 185, pp. 34, 1976.
- [37] M. D. Pedley, and Hill R., "Corrosion of Typical Orbiter Electronic Components Exposed to Halon 1301 Pyrolysis Products," National Aeronautics and space Administration, White Sands Test Facility, Las Cruces, New Mexico TR-339-001, November 25, 1985.
- [38] R. L. Alpert, "Incentive For Use of Misting Sprays As a Fire Suppression Flooding Agent," presented at Water Mist Fire Suppression Workshop, March 1-2, 1993: Proceedings, 1993.
- [39] A. T. Hills, Terence Simpson, and David P. Smith, "Water Mist Fire Protection Systems for Telecommunication Switch Gear and Other

- Electronic Facilities," presented at Water Mist Fire Suppression Workshop, March 1-2, 1993: Proceedings, 1993.
- [40] T. Eklund, "Research Needs Panel Summary," presented at Water Mist Fire Suppression Workshop, March 1-2, 1993: Proceedings, 1993.
- [41] J. R. a. J. K. R. Mawhinney, "Status Report on Water Mist Fire Suppression Systems," presented at Thirteenth Meeting of the UJNR Panel on Fire Research and Safety, March 13-20, 1996, 1996.
- [42] K. B. McGrattan, Glenn P. Forney, Jason E. Floyd, Simo Hostikka, and Kuldeep Prasad, *Fire Dynamics Simulator (Version 3) -- User's Guide. Technical Report NISTIR 6784*, 2002 ed. Gaithersburg, Maryland: National Institute of Standards and Technology, November 2002.
- [43] Building and Fire Research Laboratory, "NIST Fire Dynamics Simulator (FDS) and Smokeview." Gaithersburg, Maryland: National Institute of Standards and Technology, 2004.
- [44] G. P. Forney, and Kevin B. McGrattan, *User's Guide for Smokeview Version 3.1 -- A Tool for Visualizing Fire Dynamics Simulation Data. Technical Report NISTIR 6980*, 2003 ed. Gaithersburg, Maryland: National Institute of Standards and Technology, April 2003.
- [45] K. B. McGrattan, Howard R. Baum, Ronald G. Rehm, Anthony Hamins, Glenn P. Forney, Jason E. Floyd, Simo Hostikka, and Kuldeep Prasad, *Fire Dynamics Simulator (Version 3) -- Technical Reference Guide. Technical Report NISTIR 6783*, 2002 ed. Gaithersburg, Maryland: National Institute of Standards and Technology, November 2002.
- [46] J. Quintiere, "A Perspective on Compartment Fire Growth," *Combustion Science and Technology*, vol. 39, pp. 11-54, 1984.
- [47] S. V. Patankar, *Numerical Heat Transfer and Fluid Flow*. New York: Hemisphere Publishing, 1980.
- [48] R. Akberov, Darrell W. Pepper, and Yitung Chen, "Turbulent Flow Over a Backward Facing Step Using Penalty and Equal-Order Methods," University of Nevada, Las Vegas, Nevada 2002.
- [49] K. E. Willcox, "List of Mathematical Concepts and Definitions," Massachusetts Institute of Technology, 2002.
- [50] W. Grosshandler, Kathy Notarianni, and William Rinkinen, "Suppression Within a Simulated Computer Cabinet Using an External Water Spray," presented at Thirteenth Meeting of the UJNR Panel on Fire Research and Safety, March 13-20, 1996, 1997.
- [51] S. Nam, "Parametric Study With a Computational Model Simulating Interaction Between Fire Plume and Sprinkler Spray," Factory Mutual Research Corporation, Norwood.
- [52] B. J. Meacham, "Factors Affecting the Early Detection of Fire," in *Fire Technology*, First Quarter 1993, pp. 35.
- [53] V. Babrauskas, "Burning Rates," in *SFPE Handbook of Fire Protection Engineering, Second Edition*. Quincy, MA: National Fire Protection Association, 1995.

- [54] T. F. Barry, "Fire Exposure Profile Modeling; Some Threshold Damage Limit (TDL) Data," in *Risk-Informed, Performance-Based Industrial Fire Protection. An Alternative to Prescriptive Codes*: TFBarry Publications, 2003, pp. 1-33.

Appendices

Appendix A

Fire Factors Affecting Human Tenability [54]

Radiant Heat

Exposure at Different Incident Levels of Thermal Radiation

Radiant Heat (kW/m ²)	Human Exposure Limits*
35 to 37.5	100% lethality in 1 min; 1% lethality in 10 seconds
25.0	100% lethality in 1 min; significant injury in 10 seconds
12.5 to 15.0	1% lethality in 1 min; first-degree burns in 10 seconds
9.5	Pain threshold reached after 8 seconds; second-degree burns after 20 seconds
4.0 to 5.0	Sufficient to cause pain to personnel if unable to reach cover within 20 seconds; however, blistering of the skin (second-degree burns) is likely; 0% lethality
1.6	Causes no discomfort for long exposure

* With exposed skin

Expected Damage for Various Thermal Radiation Levels (kW/m²)

Exposure	U.S. DOT	U.K.	New South Wales
1. Causes pain after 1 min of exposure	—	—	2.1
2. Will cause pain in 15 to 20 seconds and injury (second-degree burns) after 30 seconds	5	6.3	4.7
3. Significant chance of fatality for extended exposure; high chance of injury after exposures of less than 30 seconds. Building made of cellulosic materials may suffer minor damage after prolonged exposure	12.5	10	12.6
4. Extended exposure results in fatality; there is a chance of fatality for instantaneous exposure. Buildings that are made of cellulosic materials or not fire resistant will suffer damage after short exposures. Fire-resistant structures and metal may suffer damage after prolonged exposure	21.0	—	23.0
5. Significant chance of fatality for people with instantaneous exposure. Fire-resistant structures suffer damage after short duration. Buildings of cellulosic materials ignite spontaneously. Metal fatigue after short to medium exposure	31.5	—	35.0

Convective Heat Exposure

Temperature	Effect
260°F	Difficult breathing
300°F	Mouth breathing very difficult, temperature limit for escape
320°F	Rapid, unbearable pain with dry skin
360°F	Irreversible injury in 30 seconds
400°F	Respiratory system tolerance time less than 4 min with wet skin

Oxygen Depletion

Effects of Oxygen Depletion

Percent of Oxygen in Air	Symptoms
20	Normal
17	Respiration volume increases, muscular coordination diminishes, attention and thinking clearly requires more effort
12 to 15	Shortness of breath, headache, dizziness, quickened pulse, efforts fatigue quickly, muscular coordination for skilled movements lost
10 to 12	Nausea and vomiting, exertion impossible, paralysis of motion
6 to 8	Collapse and unconsciousness occurs
6 or below	Death in 6 to 8 min

Four Stages of Asphyxiation

Stage	Percent Oxygen by Volume	Symptoms
1 st	21 to 14%	Increased pulse and breathing rate with disturbed muscular coordination
2 nd	14 to 10%	Faulty judgment, rapid fatigue, and insensitivity to pain
3 rd	10 to 6%	Nausea and vomiting, collapse, and permanent brain damage
4 th	Less than 6%	Convulsion, breathing stopped, and death

Toxic Products of Combustion

Rule-of-Thumb for Carbon Monoxide (CO) hazard:

- Concentration (ppm) x Time (minutes) > approx. 30,000 ppm-min is likely dangerous

Limiting Conditions for Toxic Products of Combustion

Chemical Products	5-Min Exposure		30-Min Exposure	
	Incapacitation	Death	Incapacitation	Death
Carbon monoxide	6000 ppm	12,000 ppm	1400 ppm	2500 ppm
Low oxygen	< 13%	< 5%	< 12%	< 7%
Carbon dioxide	> 7%	> 10%	> 6%	> 9%

Visibility Through Smoke

Proposed minimum visibility requirements for egress:

- 3 meters in primary fire compartment
- 10 meters in escape route

Appendix B

Summary of Advantages and Disadvantages of Different Fire Extinguishing Systems [30]

Water Sprinkler System	
Advantages	Disadvantages
<ul style="list-style-type: none">• Cools the equipment• Completely safe for the environment and personnel• Often less expensive to install and use• Often uses only one system throughout a building• The release of water can be localized to where it is needed	<ul style="list-style-type: none">• Impurities in the water may ruin computer microchips and other equipment• Electrical danger may exist if an automatic electricity cut-off system has not been installed• Sprinklers usually do not activate until the temperature reaches 135°F, when damage to electronic components, magnetic tape, and disks may already have occurred• May not reach a fire located within a cabinet or piece of equipment• It can be difficult or impossible to restore equipment and recover data after sprinklers have been operated

Halon 1301 System

Advantages

- Extinguishes fire without damaging computer hardware or software
- Does not conduct electricity
- Puts out fires inside equipment and furniture and in areas that a water sprinkler cannot easily reach
- The computer room can be fully operational within a couple of hours after the fire has been extinguished

Disadvantages

- Halon compounds contribute to the destruction of the ozone layer
 - Can be a health hazard, particularly to personnel suffering from asthma or heart problems
 - Release of the gas is extremely powerful, strong enough to throw equipment off desks, bring down false ceilings, and smash windows
 - It may take considerable time to gain approval for the installation of Halon 1301, because of the environmental concerns
 - Can be expensive
 - The fire may reignite if the gas is evacuated prematurely from the fire site
 - The gas fills the entire room in which the fire is located
-

Appendix C

Partial Listing of Water Misting Technology Interest [38]

Group	Location
Civil Aviation Authority	U.K.
Darchem Engineering	U.K.
FAA Technical Center	Atlantic City, NJ
Factory Mutual Research	Norwood MA
Fire Research Station	U.K.
DEC Avionics	U.K.
Greenwich University	U.K.
IEI	Australia
Kidde-Fenwal	USA
Kidde-Graviner	U.K.
Marrioff	Finland
NRC-Canada/NFL	Canada
NRL	Washington, D.C.
Securiplex Technology	Canada
SINTEF	Norway
Southbank Polytechnic	U.K.
SP	Sweden

Appendix D

FDS Variable Descriptions [45]

Symbol	Description
c_p	Constant pressure specific heat
D	Diffusion coefficient
\mathbf{f}	External force vector (excluding gravity)
\mathbf{g}	Acceleration of gravity
H	Total pressure divided by the density
k	Thermal conductivity; suppression decay factor
\dot{m}''	Production rate of i th species per unit volume
M_i	Molecular weight of i th gas species
p	Pressure
p_0	Background pressure
\mathbf{q}_r	Radiative heat flux vector
\dot{q}''	Heat release rate per unit volume
\mathcal{R}	Universal gas constant
T	Temperature
t	Time
τ	Viscous stress tensor
$\mathbf{u} = (u, v, w)$	Velocity vector
Y_i	Mass fraction of i th species
ρ	Density
$\boldsymbol{\omega} = (\omega_x, \omega_y, \omega_z)$	Vorticity vector

Appendix E

FDS Default Parameter File Listing for Central K-11 Sprinkler [42]

MANUFACTURER	<i>Manufacturer Information</i>
Central	
MODEL	<i>Sprinkler Model</i>
K-11	
OPERATING_PRESSURE	<i>Sprinkler operating pressure in units of bar.</i>
1.30	
K-FACTOR	<i>K-Factor of sprinkler in units of L/min/(bar)^{1/2}. (Default 166) The flow rate will be given by $m_w = K\sqrt{p}$ where m_w is the flow rate in L/min, K the K-factor in L/min/(bar)^{1/2} and p the gauge pressure in bar</i>
166.	
RTI	<i>Response Time Index of the sprinkler in units of pm·s. (Default 165.)</i>
148.	
C-FACTOR	<i>C-Factor of sprinkler in units of pm/s. (Default 0)</i>
0.7	
OFFSET_DISTANCE	<i>Distance in meters from the sprinkler orifice where the water droplets are initialized. It is assumed that beyond the OFFSET DISTANCE the droplets have completely broken up. (Default 0.10 m)</i>
0.20	
ACTIVATION_TEMPERATURE	<i>Link activation temperature (C). (Default 74°C)</i>
74.	
SIZE_DISTRIBUTION	<i>Information about the droplet size distribution.</i>
1	
900.,2.43,0.58	
VELOCITY	<i>Description of the initial droplet velocity distribution.</i>
1	
30. 80. 10.0	

Appendix F

Sample FDS Input File Listings

Vent Unsuppressed

&HEAD CHID='thesis',TITLE='Computer Cabinet – VentUnsuppressed' /

* Dimensions 2.5m wide x 3.0m deep x 3.0m tall

&PDIM XBAR=2.50,YBAR=3.00,ZBAR=3.00 /

* 50 cells wide x 60 cells deep x 120 cells tall = 360,000 cells

* cells 0.05m x 0.05m x 0.025m

&GRID IBAR=50,JBAR=60,KBAR=120 /

* time when finished = 1200 s

&TIME TWFIN=1200. /

* reaction is MMA, default surface is 'CONCRETE'

* data saved every TWFIN/NFRAMES = 1200s/2400 = 0.5 s

&MISC REACTION='MMA',NFRAMES=2400,SURF_DEFAULT='CONCRETE',

 DATABASE='c:\nist\fds\database3\database3.data' /

* Fire called 'HEATER' with output = 4000 kW/m²

* Worst-case scenario 10kW fire

* Heater surface .05m x .05m = approx. 0.0025 m² => approx. 10kW fire

&SURF ID='HEATER',HRRPUA=4000. /

* Creates vent with properties of 'HEATER'

* .05m wide x .05m deep on circuit board 1 (lowest)

&VENT XB=1.275,1.325,1.00,1.050,0.215,0.215,SURF_ID='HEATER' /

* COMPUTER CABINET

* circuit board 1

&OBST XB=1.000000, 1.600000, 1.000000, 1.600000, 0.210000, 0.215000,
SURF_ID='PMMA' / Circuit Board - 1

* circuit board 2

&OBST XB=1.000000, 1.600000, 1.000000, 1.600000, 0.425000, 0.430000,
SURF_ID='PMMA' / Circuit Board - 2

* circuit board 3

&OBST XB=1.000000, 1.600000, 1.000000, 1.600000, 0.640000, 0.645000,
SURF_ID='PMMA' / Circuit Board - 3

* circuit board 4

&OBST XB=1.000000, 1.600000, 1.000000, 1.600000, 0.855000, 0.860000,
SURF_ID='PMMA' / Circuit Board - 4

* circuit board 5

&OBST XB=1.000000, 1.600000, 1.000000, 1.600000, 1.070000, 1.075000,
SURF_ID='PMMA' / Circuit Board - 5

* circuit board 6

&OBST XB=1.000000, 1.600000, 1.000000, 1.600000, 1.285000, 1.290000,
SURF_ID='PMMA' / Circuit Board - 6

* left side

&OBST XB=0.950000, 1.000000, 1.000000, 1.600000, 0.000000, 2.000000,
SURF_ID='SHEET METAL' / Left Side

* right side

&OBST XB=1.600000, 1.650000, 1.000000, 1.600000, 0.000000, 2.000000,
SURF_ID='SHEET METAL' / Right Side

* back

&OBST XB=0.950000, 1.650000, 1.600000, 1.650000, 0.000000, 2.000000,
SURF_ID='SHEET METAL' / Back

* top

&OBST XB=0.950000, 1.650000, 1.000000, 1.650000, 2.000000, 2.050000,
SURF_ID='SHEET METAL' / Top

* THERMOCOUPLE TREE

&THCP XYZ=1.3,0.9,0.215,QUANTITY='TEMPERATURE' /

&THCP XYZ=1.3,0.9,0.430,QUANTITY='TEMPERATURE' /

&THCP XYZ=1.3,0.9,0.645,QUANTITY='TEMPERATURE' /

&THCP XYZ=1.3,0.9,0.860,QUANTITY='TEMPERATURE' /

&THCP XYZ=1.3,0.9,1.075,QUANTITY='TEMPERATURE' /

&THCP XYZ=1.3,0.9,1.290,QUANTITY='TEMPERATURE' /

* SLICE FILES

* VECTOR

&SLCF PBX=1.30000,QUANTITY='TEMPERATURE',VECTOR=.TRUE. / Center
x

&SLCF PBX=1.30000,QUANTITY='TEMPERATURE',VECTOR=.TRUE. / Center
y

&SLCF PBX=1.30000,QUANTITY='VELOCITY',VECTOR=.TRUE. / Center x

&SLCF PBX=1.30000,QUANTITY='VELOCITY',VECTOR=.TRUE. / Center y

&SLCF PBX=1.30000,QUANTITY='DENSITY',VECTOR=.TRUE. / Center x

&SLCF PBX=1.30000,QUANTITY='DENSITY',VECTOR=.TRUE. / Center y

* NON-VECTOR

* CENTER

&SLCF PBX=1.30000,QUANTITY='TEMPERATURE' / Center x
&SLCF PBX=1.30000,QUANTITY='TEMPERATURE' / Center y
&SLCF PBX=1.30000,QUANTITY='VELOCITY' / Center x
&SLCF PBX=1.30000,QUANTITY='VELOCITY' / Center y
&SLCF PBX=1.30000,QUANTITY='DENSITY' / Center x
&SLCF PBX=1.30000,QUANTITY='DENSITY' / Center y
&SLCF PBX=1.30000,QUANTITY='RADIANT_INTENSITY' / Center x
&SLCF PBX=1.30000,QUANTITY='RADIANT_INTENSITY' / Center y
&SLCF PBX=1.30000,QUANTITY='MIXTURE_FRACTION' / Center x
&SLCF PBX=1.30000,QUANTITY='MIXTURE_FRACTION' / Center y
&SLCF PBX=1.30000,QUANTITY='ABSORPTION_COEFFICIENT' / Center x
&SLCF PBX=1.30000,QUANTITY='ABSORPTION_COEFFICIENT' / Center y
&SLCF PBX=1.30000,QUANTITY='HRRPUV' / Center x
&SLCF PBX=1.30000,QUANTITY='HRRPUV' / Center y

* LEFT SIDE

&SLCF PBX=1.00000,QUANTITY='TEMPERATURE' / Left x
&SLCF PBX=1.00000,QUANTITY='VELOCITY' / Left x
&SLCF PBX=1.00000,QUANTITY='DENSITY' / Left x
&SLCF PBX=1.00000,QUANTITY='RADIANT_INTENSITY' / Left x
&SLCF PBX=1.00000,QUANTITY='MIXTURE_FRACTION' / Left x
&SLCF PBX=1.00000,QUANTITY='ABSORPTION_COEFFICIENT' / Left x
&SLCF PBX=1.00000,QUANTITY='HRRPUV' / Left x

* RIGHT SIDE

&SLCF PBX=1.60000,QUANTITY='TEMPERATURE' / Left x
&SLCF PBX=1.60000,QUANTITY='VELOCITY' / Left x
&SLCF PBX=1.60000,QUANTITY='DENSITY' / Left x
&SLCF PBX=1.60000,QUANTITY='RADIANT_INTENSITY' / Left x
&SLCF PBX=1.60000,QUANTITY='MIXTURE_FRACTION' / Left x
&SLCF PBX=1.60000,QUANTITY='ABSORPTION_COEFFICIENT' / Left x
&SLCF PBX=1.60000,QUANTITY='HRRPUV' / Left x

* BACK

&SLCF PBY=1.60000,QUANTITY='TEMPERATURE' / Back y
&SLCF PBY=1.60000,QUANTITY='VELOCITY' / Back y
&SLCF PBY=1.60000,QUANTITY='DENSITY' / Back y
&SLCF PBY=1.60000,QUANTITY='RADIANT_INTENSITY' / Back y
&SLCF PBY=1.60000,QUANTITY='MIXTURE_FRACTION' / Back y
&SLCF PBY=1.60000,QUANTITY='ABSORPTION_COEFFICIENT' / Back y
&SLCF PBY=1.60000,QUANTITY='HRRPUV' / Back y

* BOUNDARY FILES
&BNDF QUANTITY='GAUGE_HEAT_FLUX' /
&BNDF QUANTITY='BURNING_RATE' /
&BNDF QUANTITY='WALL_TEMPERATURE' /
&BNDF QUANTITY='CONVECTIVE_FLUX' /
&BNDF QUANTITY='RADIATIVE_FLUX' /

Surface Suppressed (Sprinkler at back of cabinet aimed forward)

&HEAD CHID='thesis',TITLE='Computer Cabinet – SurfaceBackAimedForward' /

* Dimensions 2.5m wide x 3.0m deep x 3.0m tall
&PDIM XBAR=2.50,YBAR=3.00,ZBAR=3.00 /

* 50 cells wide x 60 cells deep x 120 cells tall = 360,000 cells
* cells 0.05m x 0.05m x 0.025m
&GRID IBAR=50,JBAR=60,KBAR=120 /

* time when finished = 1200 s
&TIME TWFIN=1200. /

* reaction is MMA, default surface is 'CONCRETE'
* data saved every TWFIN/NFRAMES = 1200s/2400 = .5 s
&MISC REACTION='MMA',NFRAMES=2400,SURF_DEFAULT='CONCRETE',
DATABASE='c:\nist\fds\database3\database3.data',RESTART_FILE='thesis.rest
art',
 DATABASE_DIRECTORY='c:\nist\fds\database3' /

* Fire called 'HEATER' with output = 27.8 kW/m²
* Worst-case scenario 10kW fire
* Heater surface .6m x .6m = approx. 0.36 m² => approx. 10kW fire
&SURF ID='HEATER',HRRPUA=28. /

* COMPUTER CABINET
* circuit board 1
&OBST XB=1.000000, 1.600000, 1.000000, 1.600000, 0.210000, 0.215000,
SURF_IDS='HEATER','PMMA','PMMA' / Circuit Board - 1
* circuit board 2
&OBST XB=1.000000, 1.600000, 1.000000, 1.600000, 0.425000, 0.430000,
SURF_ID='PMMA' / Circuit Board - 2
* circuit board 3
&OBST XB=1.000000, 1.600000, 1.000000, 1.600000, 0.640000, 0.645000,
SURF_ID='PMMA' / Circuit Board - 3

```

* circuit board 4
&OBST XB=1.000000, 1.600000, 1.000000, 1.600000, 0.855000, 0.860000,
SURF_ID='PMMA' / Circuit Board - 4
* circuit board 5
&OBST XB=1.000000, 1.600000, 1.000000, 1.600000, 1.070000, 1.075000,
SURF_ID='PMMA' / Circuit Board - 5
* circuit board 6
&OBST XB=1.000000, 1.600000, 1.000000, 1.600000, 1.285000, 1.290000,
SURF_ID='PMMA' / Circuit Board - 6

* left side
&OBST XB=0.950000, 1.000000, 1.000000, 1.600000, 0.000000, 2.000000,
SURF_ID='SHEET METAL' / Left Side
* right side
&OBST XB=1.600000, 1.650000, 1.000000, 1.600000, 0.000000, 2.000000,
SURF_ID='SHEET METAL' / Right Side
* back
&OBST XB=0.950000, 1.650000, 1.600000, 1.650000, 0.000000, 2.000000,
SURF_ID='SHEET METAL' / Back
* top
&OBST XB=0.950000, 1.650000, 1.000000, 1.650000, 2.000000, 2.050000,
SURF_ID='SHEET METAL' / Top

* THERMOCOUPLE TREE
&THCP XYZ=1.3,0.9,0.215,QUANTITY='TEMPERATURE' /
&THCP XYZ=1.3,0.9,0.430,QUANTITY='TEMPERATURE' /
&THCP XYZ=1.3,0.9,0.645,QUANTITY='TEMPERATURE' /
&THCP XYZ=1.3,0.9,0.860,QUANTITY='TEMPERATURE' /
&THCP XYZ=1.3,0.9,1.075,QUANTITY='TEMPERATURE' /
&THCP XYZ=1.3,0.9,1.290,QUANTITY='TEMPERATURE' /

* SPRINKLERS
* Central K-11 ELO (Extra Large Opening) Sprinklers
* Alter default 0,0,-1 (downward) orientation to spray in -y direction
&SPRK XYZ=1.3 1.55 0.290,MAKE='K-11',ORIENTATION=0,-1,0 /
&SPRK XYZ=1.3 1.55 0.500,MAKE='K-11',ORIENTATION=0,-1,0 /
&SPRK XYZ=1.3 1.55 0.720,MAKE='K-11',ORIENTATION=0,-1,0 /
&SPRK XYZ=1.3 1.55 0.930,MAKE='K-11',ORIENTATION=0,-1,0 /
&SPRK XYZ=1.3 1.55 1.150,MAKE='K-11',ORIENTATION=0,-1,0 /
&SPRK XYZ=1.3 1.55 1.360,MAKE='K-11',ORIENTATION=0,-1,0 /

*****
* SLICE FILES
*****

```

* VECTOR

&SLCF PBX=1.30000,QUANTITY='TEMPERATURE',VECTOR=.TRUE. / Center
x

&SLCF PBX=1.30000,QUANTITY='TEMPERATURE',VECTOR=.TRUE. / Center
y

&SLCF PBX=1.30000,QUANTITY='VELOCITY',VECTOR=.TRUE. / Center x

&SLCF PBX=1.30000,QUANTITY='VELOCITY',VECTOR=.TRUE. / Center y

&SLCF PBX=1.30000,QUANTITY='DENSITY',VECTOR=.TRUE. / Center x

&SLCF PBX=1.30000,QUANTITY='DENSITY',VECTOR=.TRUE. / Center y

* NON-VECTOR

* CENTER

&SLCF PBX=1.30000,QUANTITY='TEMPERATURE' / Center x

&SLCF PBX=1.30000,QUANTITY='TEMPERATURE' / Center y

&SLCF PBX=1.30000,QUANTITY='VELOCITY' / Center x

&SLCF PBX=1.30000,QUANTITY='VELOCITY' / Center y

&SLCF PBX=1.30000,QUANTITY='DENSITY' / Center x

&SLCF PBX=1.30000,QUANTITY='DENSITY' / Center y

&SLCF PBX=1.30000,QUANTITY='RADIANT_INTENSITY' / Center x

&SLCF PBX=1.30000,QUANTITY='RADIANT_INTENSITY' / Center y

&SLCF PBX=1.30000,QUANTITY='MIXTURE_FRACTION' / Center x

&SLCF PBX=1.30000,QUANTITY='MIXTURE_FRACTION' / Center y

&SLCF PBX=1.30000,QUANTITY='ABSORPTION_COEFFICIENT' / Center x

&SLCF PBX=1.30000,QUANTITY='ABSORPTION_COEFFICIENT' / Center y

&SLCF PBX=1.30000,QUANTITY='HRRPUV' / Center x

&SLCF PBX=1.30000,QUANTITY='HRRPUV' / Center y

* LEFT SIDE

&SLCF PBX=1.00000,QUANTITY='TEMPERATURE' / Left x

&SLCF PBX=1.00000,QUANTITY='VELOCITY' / Left x

&SLCF PBX=1.00000,QUANTITY='DENSITY' / Left x

&SLCF PBX=1.00000,QUANTITY='RADIANT_INTENSITY' / Left x

&SLCF PBX=1.00000,QUANTITY='MIXTURE_FRACTION' / Left x

&SLCF PBX=1.00000,QUANTITY='ABSORPTION_COEFFICIENT' / Left x

&SLCF PBX=1.00000,QUANTITY='HRRPUV' / Left x

* RIGHT SIDE

&SLCF PBX=1.60000,QUANTITY='TEMPERATURE' / Left x

&SLCF PBX=1.60000,QUANTITY='VELOCITY' / Left x

&SLCF PBX=1.60000,QUANTITY='DENSITY' / Left x

&SLCF PBX=1.60000,QUANTITY='RADIANT_INTENSITY' / Left x

&SLCF PBX=1.60000,QUANTITY='MIXTURE_FRACTION' / Left x

&SLCF PBX=1.60000,QUANTITY='ABSORPTION_COEFFICIENT' / Left x

&SLCF PBX=1.60000,QUANTITY='HRRPUV' / Left x

```
* BACK
&SLCF PBY=1.60000,QUANTITY='TEMPERATURE' / Back y
&SLCF PBY=1.60000,QUANTITY='VELOCITY' / Back y
&SLCF PBY=1.60000,QUANTITY='DENSITY' / Back y
&SLCF PBY=1.60000,QUANTITY='RADIANT_INTENSITY' / Back y
&SLCF PBY=1.60000,QUANTITY='MIXTURE_FRACTION' / Back y
&SLCF PBY=1.60000,QUANTITY='ABSORPTION_COEFFICIENT' / Back y
&SLCF PBY=1.60000,QUANTITY='HRRPUV' / Back y
*****
```

```
* BOUNDARY FILES
&BNDF QUANTITY='GAUGE_HEAT_FLUX' /
&BNDF QUANTITY='BURNING_RATE' /
&BNDF QUANTITY='WALL_TEMPERATURE' /
&BNDF QUANTITY='CONVECTIVE_FLUX' /
&BNDF QUANTITY='RADIATIVE_FLUX' /
```

Vita

Jeff Krumm was born in Plantation, Florida. Jeff was accepted into the Dual-Degree Engineering program at Maryville College where he received a Bachelor of Arts degree with honors. He subsequently attended Washington University in St. Louis and earned a Bachelor of Science degree in Computer Engineering with honors. Following graduation, Jeff accepted a position with the Tennessee Valley Authority. While working full-time, he entered the graduate program in Electrical Engineering at the University of Tennessee in pursuit of a Masters of Science degree. As a member of the Society of Fire Protection Engineers, Jeff was introduced to the arena of computer fire modeling. Jeff will graduate receiving a Masters of Science with an emphasis in Electrical Engineering in August 2004. He continues to work at the Tennessee Valley Authority as a Measurement Specialist.